Universidade de Aveiro
2020

Departamento de Química

TIAGO PINTO VIEIRA

Análise de células interferidas em Fig4 e a sua função na via endocítica

Analysis of Fig4 interfered cells and its role on the endocytic pathway

Universidade de Aveiro
2020

Departamento de Química

TIAGO PINTO VIEIRA

Análise de células interferidas em Fig4 e a sua função na via endocítica

Analysis of Fig4 interfered cells and its role on the endocytic pathway

Dissertação apresentada à Universidade de Aveiro para cumprimento dos requisitos necessários à obtenção do grau de Mestre em Biotecnologia, Ramo de Biotecnologia Molecular, realizada sob a orientação científica da Doutora Luísa Seuanes Serafim, Professora Auxiliar do Departamento de Química da Universidade de Aveiro e da Doutora Simona Paladino, Professora Associada do Departamento de Medicina Molecular e Biotecnologia Médica da Universidade de Federico II, Itália

o júri

presidente	Professor Doutor Jorge Manuel Alexandre Saraiva Professor Associado da Universidade de Aveiro
arguente	Professor Doutor Bruno Miguel Rodrigues das Neves Professor Auxiliar da Universidade de Aveiro
orientadora	Professora Doutora Luísa Seuanes Serafim Professora e Auxiliar da Universidade de Aveiro

agradecimentos

Vorrei ringraziare la Professoressa Simona Paladino per la opportunitá di realizzare la mia tesi di laurea nel suo laboratório e per tutto l'aiuto, pazienza e suporto durante il tempo che sono rimasto in Napoli, e anche adesso.
Vorrei anche ringraziare i miei colleghi di laboratório e amice, Lucrezia, Valeria, Valentina e Teresa, per tutto l'aiuto, insegnamenti e amicizia,
Um obrigado à Professora Luísa Serafim por toda a ajuda, apoio e preocupação fornecida, não só durante a realização da tese, mas também durante a minha estadia Erasmus.
Um obrigado especial á Inês, por todo o apoio, motivação e paciência durante este período.
Gostaria de agradecer á minha família, por todo o apoio, ajuda e preocupação demonstrada nesta etapa.
Aos meus amigos Crisovsky, Minsky e Mums, que sempre se preocuparam e se mostraram disponíveis para me ajudar no que fosse necessário.
A minha gratidão a todos que de algum modo contribuíram e assistiram para a realização desta tese.
Por fim, um obrigado geral a todos os meus amigos presentes nos momentos mais difíceis, e todo o apoio e compreensão demonstrados.

palavras-chave Fosfoinositídeos, Fig4, Charcot-Marie-Tooth 4J, Via endocítica.

resumo

Mutações na inositol fosfatase Fig4 foram inicialmente associadas com a neuropatia Charcot-Marie-Tooth 4J (CMT4J), uma variante rara recessiva e desmielinizante de CMT com predominância variável em termos de idade e caracterizada por uma disfunção motora grave por envolvimento dos neurónios motores e sensoriais. Curiosamente, mutações *frameshift* e outros tipos de mutações *missense* foram reportadas por serem responsáveis pela síndrome Yunis-Varon e epilepsia familial com polimicrogirias, alargando o espectro de fenótipos associados com mutações *FIG4*. O Fig4 desfosforila o $PI(3,5)P_2$, abundantemente presente em endolisossomas, de modo a gerar PI(3)P. Desta forma e dependendo no tipo de célula, encontram-se vacúolos alargados, positivos em LAMP2, com aparência aguada ou preenchidos com material denso de eletrões em neurónios, músculo e cartilagem de ratos nulos em Fig4, sugerindo uma disfunção destes compartimentos. Contudo, o mecanismo patogénico permanece intangível.

Notavelmente, o sistema endossomal, responsável por encaminhar diversos tipos de vias intracelulares, emergiu e continua a emergir como elemento chave em diversas doenças neurológicas.

Esta trabalho teve como objetivo compreender o papel de Fig4 na regulação da via endossomal, de modo a elucidar os mecanismos da patogénese destas doenças neurológicas. Além disso, pertendeu-se que este estudo contribuisse para uma melhor compreensão de fosfoinositídeos como reguladores de tráfego membranar.

Desta forma, analisaram-se os efeitos do silenciamento de Fig4 na via endossomal. Através de análises de ensaios de *western blot* e de imunofluorescência, foi possivel avaliar a homeostasia e dinâmicas de compartimentos endossomais. Avaliou-se ainda o impacto do silenciamento de Fig4 no que diz respeito à viabilidade das células, efetuando curvas de crescimento. Verificou-se ainda que o silenciamento do Fig4 alterou drasticamente todo o eixo endo-lisossoma observando-se um alargamento dos lisossomas, assim como do aumento do número e alargamento dos endosomas tardios e iniciais. Além disso, os níveis de proteínas endocíticas resistentes aumentaram, sugerindo uma alteração das suas dinâmicas.

Estes resultados indicam que a atividade do Fig4 é crucial para a homeostasia e funcionamento dos compartimentos endossomais em diferentes tipos de células. A disfunção destas vías poderá constituir a base de patogénse de doenças associadas a Fig4.

.

keywords Phosphoinositides, Fig4, Charcot-Marie-Tooth type 4J, Endocytic pathway

abstract

Mutations in the inositol phosphatase Fig4 were firstly associated with Charcot-Marie-Tooth 4J (CMT4J) neuropathy, a rare recessive demyelinating form of CMT with highly variable onset and characterized by severe motor dysfunction and involvement of motor and sensory neurons. Interestingly, frameshift and other missense mutations have been reported to be responsible of Yunis-Varon syndrome and familial epilepsy with polymicrogyria extending the spectrum of phenotypes associated with *FIG4* mutations. Fig4 dephosphorylates the endolysosome enriched $PI(3,5)P_2$ to generate PI(3)P. Enlarged LAMP2 positive vacuoles with watery appearance or filled with electron dense material (depending on cell type) are found in neurons, muscle and cartilage of Fig4 null mice, suggesting a dysfunction of these compartments. However, the pathogenic mechanism(s) still remain elusive.

Strikingly, the endosomal system, which is a crossroad of distinct intracellular pathways, has emerged and is still emerging as key player in various neurological disorders.

This research aimed to understand the role of Fig4 in regulating the endosomal pathway in order to elucidate the pathomechanisms of these neurological disorders. Moreover, these analyses also intended to contribute to a better comprehension of phosphoinositide as regulators of membrane trafficking.

To this purpose, the effects of the knockdown of Fig4 expression on the endosomal pathway were analyzed. By western blot analyses and immunofluoescence assays the homeostasis and dynamics of endosomal compartments were evaluated. Furthermore, the impact of Fig4 knockdown on cell viability was studied by performing growth curves. Fig4 knockdown was found to drastically alter the whole endo-lysosome axis: lysosomes appear as large dots and also late and early endosomes are numerous and enlarged. In addition, the levels of endocytic resistant proteins are increased, suggesting an alteration of their dynamics.

These results indicate that Fig4 activity is crucial for the homeostasis and function of endosomal compartments in different cells types. The dysfunction of these pathways might underlie the pathogenesis of Fig4-associated diseases.

Index

Figure Index

Table Index

Glossary

Term	Definition
bp	Base pair
BSA	Bovine serum albumin
CMT	Charcot Marie Tooth
CMT4J	Charcot Marie Tooth 4J
COPI	Coat protein complex I
COPII	Coat protein complex II
Ctl	Scrambled RNA transfected control cells
ECL	Electrochemiluminescence
EEA1	Early endosomal auto antigen
EGTA	Egtazic acid
ER	Endoplasmic Reticulum
FBS	Fetal bovine serum
FIG4	Factor-induced gene
Fig4i	Fig4 silenced cells
GAPDH	Glyceraldehyde 3-phosphate dehydrogenase
GTP	Guanine triphosphate
HRP	Horseradish peroxidase
LAMP	Lysosomal-associated membrane protein
NP40	Nonyl phenoxypolyethoxylethanol 40
PBS	Phosphate-buffered saline
PH	Pleckstrin homology
PI(3,5)P_2	Phosphatidylinositol 3,5- bisphosphate
PI(3)P	Phosphatidylinositol 3- phosphate
PIP5K3/PIKfyve	Phosphatidylinositol 3-Phosphate 5-Kinase
PtdIns	Phosphatidylinositol
Plt	Pale tremor mice
PVDF	Polyvinylidene difluoride

RAB	Ras-associated binding
RPMI	Roswell park memorial institute
SDS-PAGE	Sodium dodecyl sulfate–Polyacrylamide gel electrophoresis
TBST	Tris-buffered saline
TGN	Trans-Golgi network
YVS	Yunis-Varon syndrome

Chapter 1

1. Brief introduction and rationale

Homeostasis of eukaryotic cells is largely dependent on dynamic compartmentalization of the endomembrane system. Proper membrane trafficking, which connects different organelles, is essential to maintain the proper composition of cellular compartments as well as to ensure their homeostasis and functions.

With respect to other cell types, the nervous system is more sensitive to defects of membrane trafficking. Indeed, in the last years many studies highlighted that several genes responsible for hereditary forms of neurological disorders are component of the machinery regulating membrane trafficking.

In humans *FIG4* gene encodes a phosphoinositide 5-phosphatase that is involved in the turnover of phoshatidylinositol-3,5-bisphospate, PI(3,5)P_2, which is enriched in late endosomes and lysosomes. Together with specific kinases, the activity of phosphatases controls the levels of phosphoinositides (PI), a class of phospholipids that have emerged as important regulators of membrane trafficking by acting as membrane designations for selective protein recruitment and assembly, thereby triggering downstream signaling cascades. Numerous findings highlighted that the levels of PI might be finely regulated, in time and in the space, and are critical for membrane homeostasis. Specifically, PI metabolism seems critical for nervous system functions.

Mutations in this gene have been associated with different human neurological diseases. *FIG4* mutations were first described in Charcot-Marie-Tooth 4J (CMT4J) patients. CMT4J is a rare and recessive demyelinating form of CMT, which is characterized by a severe motor dysfunction and loss of sensory neurons. Later, other disease-causing variants in Fig4 have been identified in patients affected with Yunis-Varon syndrome and familial epilepsy with polymicrogyria syndrome, extending the spectrum of disease phenotypes associated with *FIG4* mutations. However, the pathogenic mechanism(s) still remain elusive.

The main interest of the research group where the present thesis was developed is to unravel the role of membrane trafficking in the proper functions of nervous system as to understand how dysfunction of membrane trafficking may lead to neurodegeneration.

Chapter 2

2. State of the Art

2.1 Mendelian disorders of membrane trafficking

Almost all proteins in eukaryotic cells reach the right intracellular location with the help of sophisticated transport and delivery systems. The secretory pathway encompasses a large group of organelles (endoplasmic reticulum, Golgi complex and the endo-lysosomal stations) and is responsible for transporting about one third of the human proteome, including transmembrane and lipid-anchored proteins as well as secreted proteins, from their site of synthesis, the endoplasmic reticulum (ER), to their final destination (Figure 1) (De Matteis, 2011). The correct membrane trafficking between these organelles, is essential to maintain the proper composition of cellular compartments as well as to ensure their homeostasis (size, shape of each compartment) and functions. Moreover, membrane trafficking through exocytic and endocytic routes guarantees the exchange between cells and extracellular environment: secretion of thousands of cargo species including growth factors, matrix, serum proteins, hormones, antibodies, as well as an uptake of several nutrients crucial for cell metabolism and, as consequence, for cell viability (Figure 1) (De Matteis, 2011; Doherty & McMahon, 2009).

So far, many studies have shed light on the molecular machinery regulating membrane trafficking and about 2000 proteins have been identified as key regulators (Schekman & Rothman, 2002; De Matteis & Luini, 2008). In the last three decades, thanks to yeast genetics and biochemical identification of the relevant components in mammals, the knowledge in this area has grown profoundly (Ira, Mellman. Graham, 2000; Rothman, 2002; Schekman & Rothman, 2002). Thus, it is not surprising that alterations in membrane trafficking can result in several diseases.

The endoplasmic reticulum is the site of newly synthesized secretory proteins and where their journey begins. Proteins are glycosylated and folded by a complex machinery, involving chaperone proteins upon being inserted in the lumen of the endoplasmic reticulum (Ellgaard & Helenius, 2003). The folding process is essential for the proteins to exit from the ER, that has a molecular machinery for exerting protein control quality (Vembar & Brodsky, 2008). Well folded proteins leave the endoplasmic reticulum in small or large budding vesicles coated by protein complex II (COPII) (Watson & Stephens,

2005). Through the Golgi complex cisternae, cargo proteins and lipids undergo chemical modification, the most frequent glycosylation. The Golgi complex is also the main sorting station: through COPI carriers some cargoes are redirected back to the endoplasmic reticulum, and at the trans-Golgi network (TGN) level, different cargoes are segregated from each other and selectively incorporated in vesicles to be delivered to their correct final destination (Béthune et al., 2006; De Matteis & Luini, 2008)

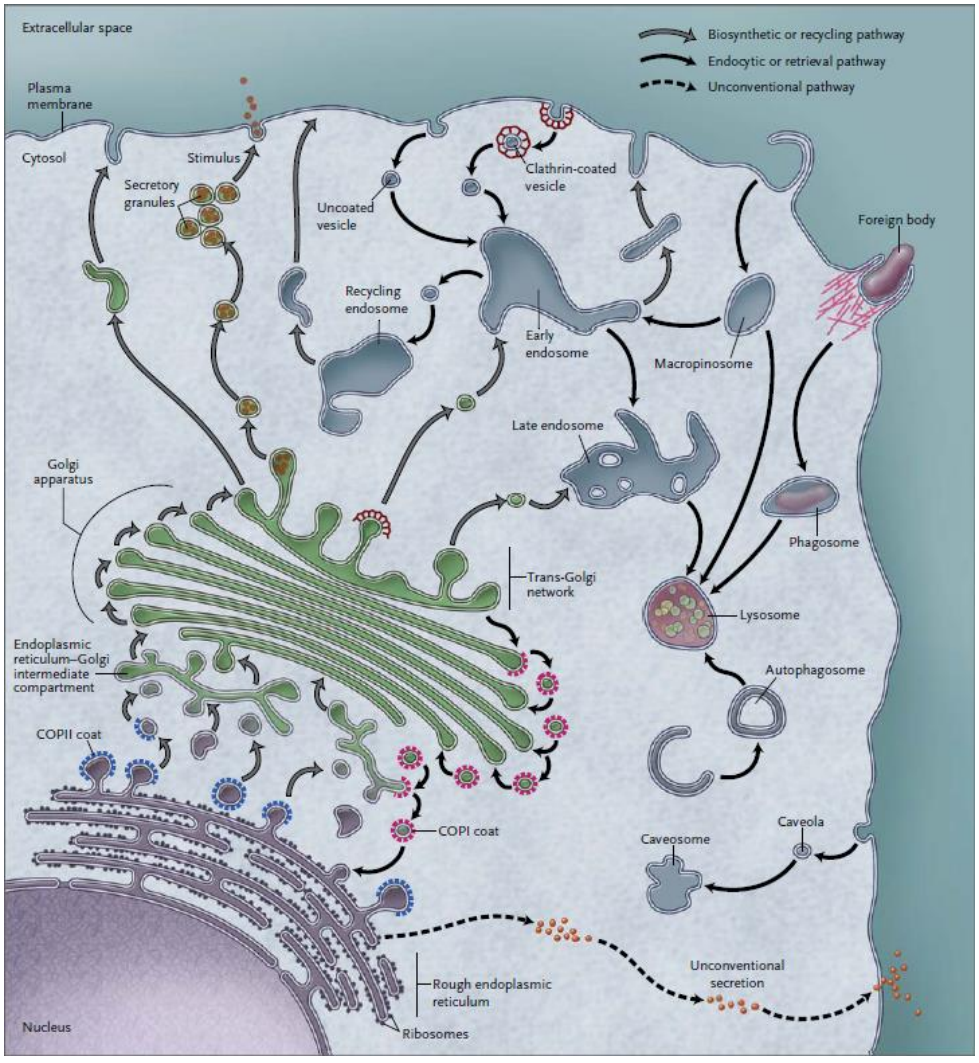

Figure 1 - Endocytic and other membrane trafficking pathways by De Matteis & Luini, 2008

At the cell surface, membrane proteins undergo endocytosis for their physiological turn over (Figure 1). Moreover, endocytosis is an important process involved in many functions, for instance, the control of the composition of the plasma membrane, uptake of essential nutrients and cell signalling (Doherty & McMahon, 2009). Most of the endocytic carriers fuse into early endosomes, a vacuolar-tubular sorting station from which cargo proteins are sorted to be delivered to distinct locations: some proteins are recycled back to the cell surface through a fast route directly to the plasma membrane or slower one through recycling endosomes; other cargo proteins can move towards the trans-Golgi network, and others are transported to late endosomes from which cargoes are transferred to lysosomes for degradation (Pryor & Luzio, 2009).

It is well established that organelles of endocytic pathway are very dynamic: there exists a process of compartment progression and maturation between early endosomes and late endosomes. In the maturation process the compartments change compositions along the transport pathway. Early endosomes mature into late endosomes undergoing a process called Ras-associated binding (RAB) conversion, switching between RAB5 and RAB7. This process is essential to endosome maturation (Rink et al., 2005). RAB proteins are a large family of small GTPases that control and coordinate multiple events including motility, maturation and fusion of vesicles through the recruitment of effector proteins. Some RABs are enriched in specific compartments and, by regulating the incoming and outgoing traffic, participate in the acquisition and maintenance of the identity of these compartments and in the spatiotemporal regulation of trafficking.

Transport systems present a large degree of redundancy and functional plasticity, which may compensate some defects. On the other hand, cell needs can be different, depending on the specific requirements for each cell type and this results in selective vulnerability of specific tissues. Trafficking systems maintain their homeostasis, despite the rapid membrane fluxes that constantly change the size and composition of the transport organelles or compartments. The maintenance of the equilibrium is possible thanks to signalling circuits located on the trafficking organelles recently discovered, that are capable of sensing the passage of traffic and rapidly react to restore the balance (Pulvirenti et al., 2008).

Over the last years, several components of molecular machinery regulating membrane trafficking have been shown to be associated with human diseases (De Matteis

& Luini, 2008; Schreij et al., 2016). Many efforts are being made to better understand the molecular basis of these diseases. Mendelian diseases of the membrane trafficking have been associated to mutation in genes encoding for cargo proteins or components of the biosynthetic and trafficking machinery. Genes from cargo proteins appear to represent a bigger number, since they are more numerous and many cargoes are tissue specific and not essential for the survival of an embryo (Winter et al., 2004). Mutation in genes that encode ubiquitous transport-machinery proteins are more likely to be lethal and some of these mutations can be partially compensated thanks to the plasticity of the transport system.

When cargo proteins are mutated, a pathogenic chain of events may occur involving either a loss of function because of protein truncation or its early degradation, or even a gain of function, which might lead to excessive unfolded protein response activation (Ron & Walter, 2007). If the amount of misfolded cargo exceeds the capacity of the compensatory mechanisms, activated through the unfolded-protein response, the response becomes detrimental and triggers cell damage and death, event that usually occurs at disorders of myelinating cells. (Lin & Popko, 2009).

Regarding mutations in the machinery proteins, it is unknown how defects in overall conserved housekeeping components can give rise to manifestations that are often specific to an organ or a tissue. In some cases, the defective genes are predominantly expressed as specific isoforms in the affected tissues explaining the tissue vulnerability. Another possibility is a high request of the defective genes, in relation to the specific needs of the tissue: some cells/tissues' functions are dependent on trafficking pathways, and therefore, the rate of these pathways is also important for them (e.g., Schwann cells strictly depend on the efficient secretory pathway for myelination).

The better understanding of molecular mechanisms regulating membrane trafficking can give insights regarding the pathogenesis of mendelian diseases and develop new therapies. On the other hand, the study of mendelian diseases may shed new insights on the molecular machinery functions. Interestingly, mendelian disorders, despite originated from different gene mutations, may share overlapping clinical phenotype and this can help the discovery of converging molecular pathways (Vicinanza et al., 2008).

2.2 Phosphoinositides

Lipids are biomolecules that have essential roles in regulating membrane trafficking as well as important roles in cell motility, adhesion and signal transduction. (Berridge & Irvine, 1989; Martin, 1998) Among them, phosphoinositides (PIs), phosphatidylinositol derivatives, are a class of lipids characterised for being short lived and phosphorylated (De Matteis & Godi, 2004; Di Paolo & De Camilli, 2006). Although, they comprise less than 5% of total cellular lipids, PIs are essential components of cellular membranes and play key roles in many fundamental biological processes (Di Paolo & De Camilli, 2006; Mayinger, 2012; Shewan et al., 2011).

Like other phospholipids, they consist of a glycerol backbone, which is esterified by two fatty acids and a phosphate that is attached to a polar head group, the cyclic polyol myoinositol. The phosphatidylinositol (PtdIns), the precursor of phosphoinositides, is synthesized primarily in the endoplasmic reticulum and is then delivered to other membranes, either by vesicular transport or via cytosolic PtdIns transfer proteins (Di Paolo & De Camilli, 2006). Reversible phosphorylation of the myo-inositol head group at position 3, 4 and 5 gives rise to seven PI isoforms identified in eukaryotic cells: PI(3)P, PI(4)P, PI(5)P, PI(3,4)P_2, PI(3,5)P_2, PI(4,5)P_2 and PI(3,4,5)P_3 (Figure 2).

Conversion between these isoforms is controlled by specific phosphoinositide kinases and phosphatases that regulate the balance of these lipids (Figure 2). The concerted action of PI kinases and phosphatases that attach or remove phosphate groups respectively, and phospholipases, that cleave lipids, results in the generation of unique PI enrichment in distinct intracellular membranes (Di Paolo & De Camilli, 2006; Krauß & Haucke, 2007; Stenmark, 2003). Therefore, PIs can serve as a unique lipid signature or code, like RAB proteins, for cellular organelle identity (Figure 2). Furthermore, within a given membrane, the localization of specific phosphoinositides can be heterogeneous, thus identifying specific sub-domains (Figure 2). Hence, the differential intracellular distribution of phosphoinositides, together with their high turnover, makes these lipids key mediators of signaling events in all cellular compartments (Di Paolo & De Camilli, 2006; Krauß & Haucke, 2007).

By acting as membrane designations for selective protein recruitment and assembly, PIs may trigger downstream signaling cascades. In particular, through the

binding of their head groups to cytosolic proteins or cytosolic domains of membrane proteins they can regulate the function of integral membrane proteins (such as ion channels, and transporters), or recruit to the membrane cytoskeletal and signaling components (Di Paolo & De Camilli, 2006; Falkenburger et al., 2010; Xiaoli Zhang et al., 2012). Moreover, PIs are responsible for controlling the correct timing and location of many trafficking events (De Matteis, 2011; Di Paolo & De Camilli, 2006). They have been also found to be involved in the regulation of the cytoskeleton, nuclear events and membrane permeability.

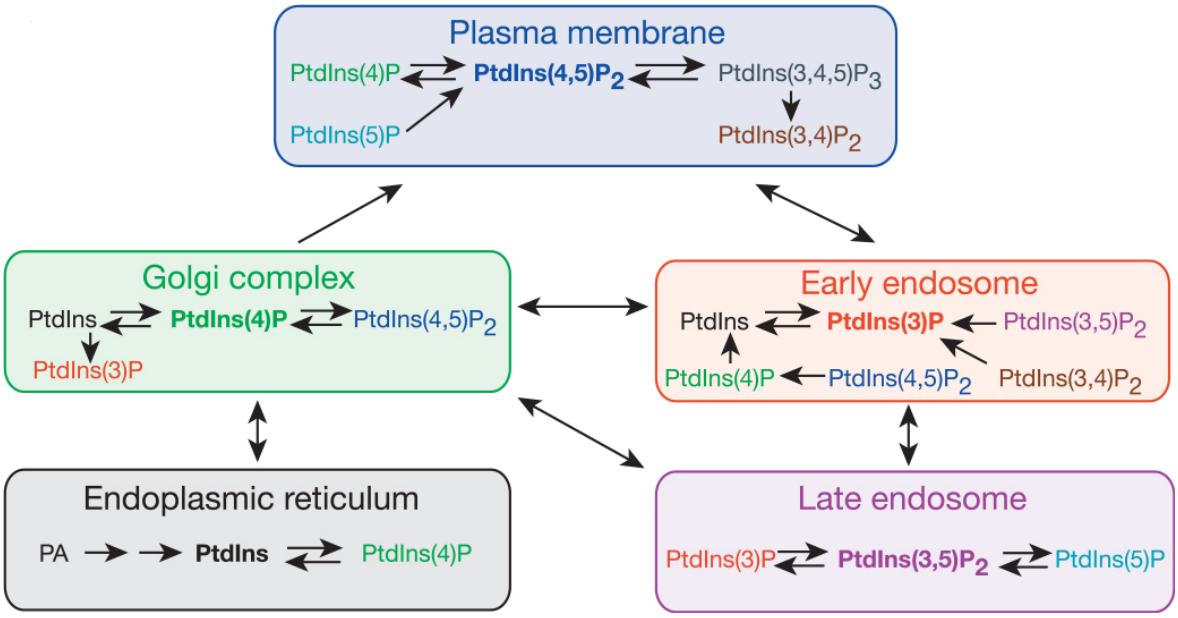

Figure 2 - All phosphoinositide species and their interactions and locations by Di Paolo & De Camilli, 2006

Typically, the binding of proteins to phosphoinositides involves electrostatic interactions with the negative charges of the phosphate(s) on the inositol ring. In some cases, adjacent hydrophobic amino acids strengthen that interaction (Lemmon, 2003). Proteins that interact with phosphoinositides can consist either of clusters of basic residues within unstructured regions, such as those found in many actin regulatory proteins (Yin & Janmey, 2003), or of folded modules, such as the pleckstrin homology (PH) domain (Balla, 2005; Lemmon, 2003).

As aforementioned, the endosomal pathway is a dynamic system of membranes that connects traffic to and from the plasma membrane, the Golgi complex and the lysosomes (Odorizzi et al., 2000). Several studies highlighted the crucial role of PI(3)P and PI(3,5)P_2

for endosomal compartments, being involved in membrane remodelling and trafficking (Banta et al., 1990; Yamamoto et al., 1995). Nevertheless, there is not much information regarding regulation of mammalian PI(3,5)P_2, a small phospholipid present in small quantities and located on the cytosolic surface of membranes of the late endosomal compartment responsible for regulating membrane trafficking in the endosome-lysosome pathway in yeast (L. Volpicelli, 2007; Michell et al., 2006).

PI(3,5)P_2 was first described in yeasts where its synthesis is strongly induced by osmotic stress, and was also discovered as a minor lipid component in non-stimulated mammalian cells (Dove et al., 1997; Whiteford; et al., 1997). With respect to other PIs, it is present in very low concentration (only 0.04/0.08% of total PI). The presence of this PI is dependent on the action of PI(3)P kinase PIKfyve and the phosphatase Fig4, that form a ternary complex with the adaptor protein ArPIKfive (Jin et al., 2008). The PI(3,5)P_2 is enriched in the late compartments of the endosomal pathway (late endosomes, multivesicular bodies, lysosomes) (Di Paolo & De Camilli, 2006).

It is not surprising that PIs are emerging to be involved in many cellular processes such as membrane trafficking, cytoskeleton remodelling and signalling. The spatiotemporally regulated production and turnover of PIs is critical for PI functions. As aforementioned, this is achieved by strict control of the subcellular distribution, membrane association and activity state of each of different kinases and phosphatases. Confirming their crucial role in cells, mice with mutation in the kinases or phosphatases that regulate levels of PIs, die during embryonic life or develop severe neurological defects (Di Paolo & De Camilli, 2006; Vicinanza et al., 2008). An increasing number of human genetic diseases including myopathies and neuropathies are associated to mutations in enzymes regulating the turnover of PIs (Nicot & Laporte, 2008; Waugh, 2015).

2.3 Fig4: an inositol phosphatase

In humans *FIG4* gene is located on chromosome 6 (from base pair 109,691,221 to base pair 109,825,43). It encodes a lipid phosphatase of 103 kDa comprised of 907 amino acids, the Fig4 protein, also known as SAC domain-containing protein 3 (Sac3) (Chow et al., 2007). Fig4 belongs to the family of enzymes (from lower to higher eukaryotes), containing a conserved phosphoinositide (PI) phosphatase module termed Sac (suppressor of actin) domain (Hughes et al., 2000). Fig4 was originally identified in a screen for genes induced by mating pheromone in Saccharomyces cerevisiae (Erdman et al., 1998). The mammal protein is closely related to the yeast one, with overall amino acid sequence identity of 35% and similarity of 66% (Chow et al., 2007). The Sac domain comprises about 500 amino acids and contains seven highly conserved motifs including the CX5R(T/S) catalytic motif, which is essential for catalytic activity (Hughes et al., 2000). Like in yeasts, in humans there are also five Sac phosphatase domain containing proteins, which appear to fall into two subfamilies. Members of the first subfamily, including the transmembrane protein Sac1, cytosolic proteins Sac2/INPP5f and Sac3/Fig4, have an N-terminal Sac phosphatase and no other recognizable structural domains. The second subfamily comprises two synaptojanin homologues, which have a PI 5-phosphatase domain immediately after the N-terminal Sac phosphatase module (Hughes et al., 2000). Each Sac phosphatase prefers a specific subgroup of PIs as substrates, although how the substrate specificity is determined is still not very clear. Specifically, Fig4 removes the 5-phosphate from the phosphoinositide PI(3,5)P_2 to generate PI(3)P both in vitro and in vivo (Duex et al., 2006; Simon A. Rudge, Deborah M. Anderson, 2004). Consistently with public expressed-sequence-tag and microarray databases, RT-PCR of tissues from wild type mice showed widespread expression of Fig4 (Chow et al., 2007). Moreover, transcript appears distributed throughout the brain as revealed by in situ hybridization (Chow et al., 2007).

2.3.1 Structure and enzymatic activity

Structural studies of Fig4/SAC3 have not yet been performed, but important information has been inferred through the crystal structure of the founding member of this

family, the Sac1p, which is the only crystal structure solved in this family (Manford et al., 2010). The Sac domain of yeast Sac1p comprises two closely packed sub-domains: a N-terminal subdomain (SacN domain; residues 1-182) and a C-terminal domain of about 320 residues in which is present the catalytic site CX5R(T/S) (Manford et al., 2010). The SacN domain comprises three layers of β-sheets and one long and three short α-helixes. The SacN domain is closely opposed to the catalytic domain, but it takes some contacts through its third layer (Manford et al., 2010). The function of this domain is still unknown, but it may control the enzymatic function through interactions with other unknown factors. The catalytic domain consists of a nine-stranded and partially split β-sheet that is flanked by five α-helixes with two on one side and three on the other. The catalytic site (residues 392-399) is constituted by a conserved cysteine (Cys) followed by 5 amino acids and arginine (Arg) forming a conserved loop (termed P-loops). Finally, five protruding loops surrounding the catalytic site (Manford et al., 2010).

Through a conserved mechanism in yeast and in mammals, Fig4 formed a ternary complex (Figure 3) with PIKfyve (Fab1 in yeast) and the ArPIKfyve adaptor protein (Vac14 in yeast), which regulates both the kinase and phosphatase activities(Ho et al., 2012; Jin et al., 2008). Yet, it is not completely clear the dynamics through which this complex is formed and then performs its function, nor how it is regulated. Various studies suggest that Fig4 could bind Vac14/ArPIKfyve before binding the kinase Fab1/PIKfyve efficiently (Botelho, 2008; Ikonomov et al., 2009; Sbrissa et al., 2007).

This complex is responsible for the acute regulation of subcellular levels of $PI(3,5)P_2$ (Botelho, 2008; Jin et al., 2008; Sbrissa et al., 2008). Similarly to the deficit of Fig4, the loss of Fab1, which is lethal in some eukaryotes such as C. elegans and Drosophila, induces the formation of an enlarged, swollen vacuole in yeast cells (Efe et al., 2005) or the loss of ArPIKfyve in mice leads to massive neurodegeneration with accumulation of LAMP-2 positive vacuoles (Y. Zhang et al., 2007). All together these findings indicate that the levels of $PI(3,5)P_2$ might be finely regulated and are critical for membrane homeostasis and specific for the survival of neural cells. How the function of Fig4 is impaired in the disease mutants is still not understood since pathological mutations are mapped outside of the catalytic site.

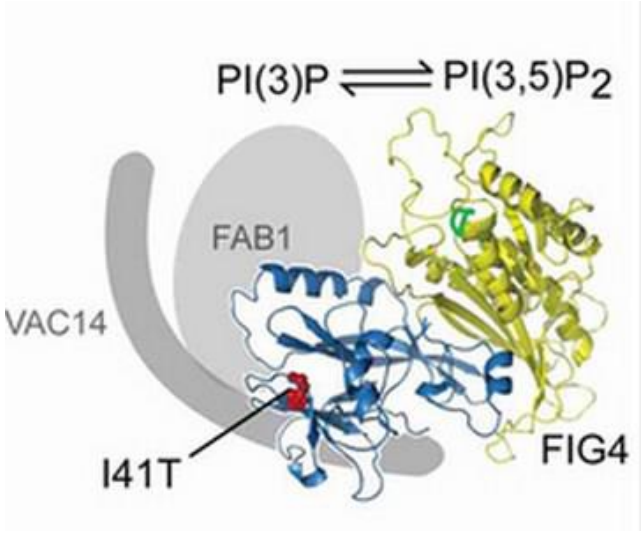

Figure 3 - The ternary complex containing Fig4, PIKfyve (FAB1) and ArPIKfyve (VAC14) regulates the overall concentration of $PI(3,5)P_2$ by Lenk, 2011

2.4 Fig4 associated diseases: Charcot-Marie-Tooth 4J, Yunis-Varon syndrome and familial epilepsy with polymicrogyria

2.4.1 Charcot-Marie-Tooth 4J

Four unrelated patients with hereditary motor and sensory neuropathy have been identified with a pathogenic mutation in human *FIG4* on chromosome 6q21. The pathogenic mutation revealed to cause the recent form of autosomal recessive Charcot-Marie-Tooth disorder, CMT type 4J (CMT4J) (Chow et al., 2007). CMT4J is a rare recessive demyelinating form of CMT with the involvement of both sensory and motor neurons (Chow et al., 2007).

CMT4J patients are compound heterozygotes with a null allele in combination with the partial loss-of-function missense mutation I41T (Chow et al., 2007; Nicholson et al., 2011; Zhang et al., 2008).

At a clinical level, CMT4J is characterized by severe motor dysfunction with rapid clinical progression that results in weakness, often asymmetric, of proximal and distal muscles. The disease shows a clinal progression of an active denervation with massive fibrillations and an uneven distribution of vacuolated motor neuron in the spinal cord, which may explain the asymmetric progression in patients. Initially, the CMT4J phenotype

was described as a severe early onset CMT (Chow et al., 2007), but further studies showed that the CMT4J was characterized by a highly variable onset (from early childhood to the sixth decade), and severity (Tazir et al., 2013).

Moreover, it has been observed that, beyond the motor neurons, sensory neurons are also affected (Chow et al., 2007; Zhang et al., 2008). In fact, CMT4J patients exhibit, albeit slight, sensory abnormalities such as reducing the sensitivity of the distal limbs and decreased tendon reflex (Saporta et al., 2011; Tazir et al., 2013). On neurological examination, dysfunction of the cranial nerves is uncommon and these patients usually display normal cognitive function.

At histological level, sural nerve biopsies of CMT4J patients show extensive loss of large-diameter myelinated fibers and onion bulb lamellae surrounding some remaining demyelinating fibers (Figure 4) (Nicholson et al., 2011; Zhang et al., 2008). There is relative sparing of moderate to small diameter fibers, which range from thinly myelinated to absent myelin. These features are also seen in the sciatic nerve of pale tremor (plt) mice, an animal model of this disease (Chow et al., 2007).

Hence, the defects in myelin sheath formation could imply the involvement of glial cells in the pathogenesis of disease. This is supported by recent findings showing that mice with conditional inactivation of Fig4 in Schwann cells display demyelination (Vaccari et al., 2014).

At the cellular level, plt mice display: i) enlarged vacuoles with watery appearance immunoreactive for the late endosomes/lysosomes protein LAMP-2 in sensory neurons (Chow et al., 2007; Cole J. Ferguson et al., 2009); ii) enlarged Lamp-1/2 positive endo-lysosomes filled with electron dense material (Chow et al., 2007; Katona et al., 2011) in spinal motor/cortical neurons and glia. LAMP-2 reactive vacuoles accumulation is also observed in fibroblasts from patients with CMT4J (Zhang et al., 2008). Thus, it appears that the deficiency of Fig4 leads to wide expansion and, probably, to dysfunction of the late endosome/lysosome compartments. Moreover, the observed differences of the cellular phenotype in the different types of neurons suggest that Fig4 might have different roles in the diverse cell types possibly by controlling specific cell pathways.

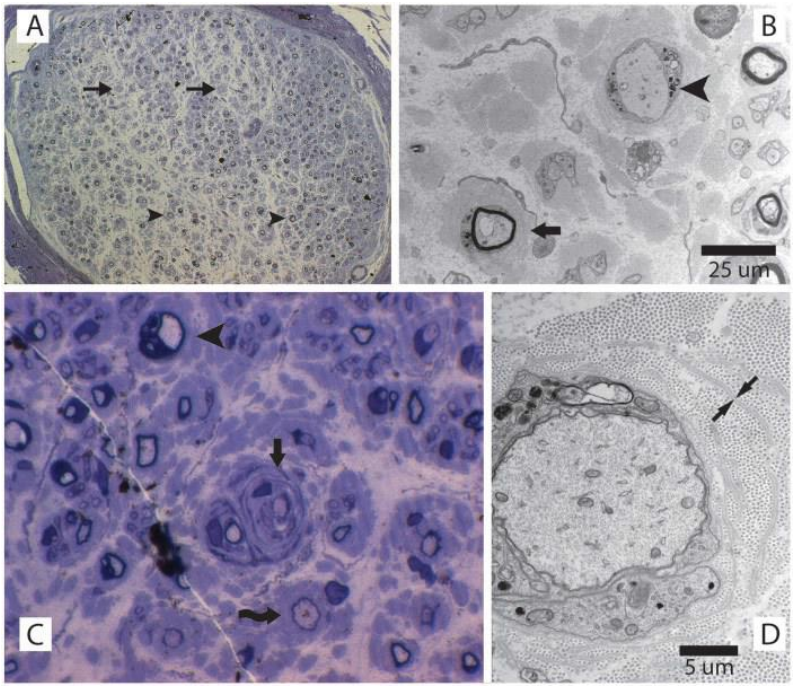

Figure 4 - Sural nerve biopsy of a patient with CMT4J. Anomalies in myelinated fibers are detected in a sural biopsy of CMT4J patient. (A) Cross section of a sural nerve fascicle with extensive loss of large myelinated fibers. (B) Electron microscopy demonstrating one naked axon with myelin breakdown products (arrowhead) and one thinly myelinated axon with surrounding onion bulb remnants and no clear Schwann cell processes (arrow). (C) Thinly myelinated axon with multiple thin myelin bands within the surrounding onion bulb (arrow). Also visible, a demyelinated axon (arrowhead) and a thinly myelinated axon (curving arrow). (D) Electron microscopy demonstrating a minimally myelinated axon with myelin breakdown products. Arrows indicate the cell remnants of a Schwann cell (from Nicholson et al. 2011)

2.4.2 Yunis-Varon syndrome

Fig4 is also related to other neurological diseases like Yunis-Varon syndrome (YVS). By exome sequencing of individuals affected by YVS, mutations of *FIG4* were found in three families (Campeau et al., 2013). The genotype of YVS is heterogenous. In the first family, consanguineous parents carried the same frameshift mutation, a deletion of 2 base pair (bp) (c.1260_1261delGT), which causes a truncation of the protein upstream of the catalytic domain and therefore a complete loss of function of the protein. In the second family, the maternal allele carried the missense mutation Gly104Asp and the paternal allele a deletion of 8 bp (c.831_838delTAAATTTG). The affected child was a compound heterozygote for the two mutations. In the third family, with no reported consanguinity, both parents were carriers of the Leu175Pro missense mutation and the affected child was homozygous for the mutation. The missense mutations Gly104Asp and Leu175Pro represent highly conserved amino acid residues during evolution. Four programs of protein structure prediction have estimated that these two missense mutations can influence the function of Fig4.

Analysis of a patient fibroblasts revealed the presence of large vacuoles as well as electrondense inclusions. The histological examination of the muscles revealed fibers that vary in size and rich in enlarged vacuoles (Campeau et al., 2013).

Contrary to CMT4J presenting a partial Fig4 activity, YVS display a complete loss of Fig4 activity and this might reflect in the severe clinical phenotype of YVS, which is characterized by dysfunction of central nervous system and extensive skeletal anomalies.

In Figure 5, mutations in *FIG4* gene responsible for causing YVS and CMT4J are shown (Campeau et al., 2013; Varghese et al., 2014). A deep study structure-function of Fig4 comparing the different pathological mutants will be the next challenge to elucidate the molecular mechanisms of the two diseases.

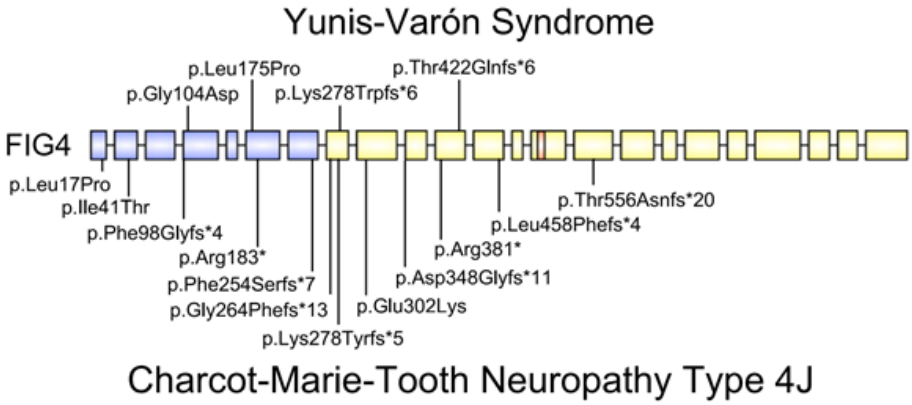

Figure 5 - Mutations of Fig4 exons (introns not drawn to scale) causing CMT4J (below) and YVS (above) fall in different domain of Fig4: protein interaction domain (blue) and catalytic domain (yellow). by Campeau, 2013

2.4.3 Familial epilepsy with Polymicrogyria

As referred before, *FIG4* mutations are implicated in the neuropathies CMT4J and YVS. (Campeau et al., 2013) Nevertheless, Fig4 has also been associated with Familial epilepsy with polymicrogyria, a malformation of the cerebral cortex characterized by abnormal lamination and folding. The misinformation of the Fig4 role has been a problem in the understating of how *FIG4* mutation can lead to such distinct autosomal recessive disorders. CMT4J a neuropathy only affecting the peripheral nervous system, (Piao et al., 2004) YVS associated with neurodegeneration and brain malformations which are related to cleidocranial dysplasia, digital anomalies and early death, (Valence et al., 2013) and temporo-occipital polymicrogyria with seizures and psychiatric features. As referred before, YVS presents a null mutation of *FIG4*, homozygous or compound heterozygous, whilst alike CMT4J, polymicrogyria retains a partial Fig4 function. The total loss of function presented in YVS impedes the rescue of vacuolization by Fig4-null fibroblasts. (Campeau et al., 2013) Spongiform neurodegeneration is exclusive to complete loss of Fig4 function in pale tremor mice and patients with YVS. CMT4J does not exhibit this particular neurodegeneration since I41T mutation only has a partial loss of function, and the protein overexpression is enough to present the cell Fig4 residual function and rescue it from lethality. (Chow et al., 2007; Lenk et al., 2011; Nicholson et al., 2011) *FIG4* mutations may have some phenotypic overlap, in example patients with YVS, besides presenting brain malformations, also include underdeveloped gyri and polymicrogyria, characteristic of p.Asp783Val mutation phenotype. (Kulkarni et al., 2006; Walch et al., 2000) It was observed that a patient with YVS did not overlap the neuronal vacuolization phenotype with the areas exhibiting pachygyria and polymicrogyria, which may indicate that the neurodegeneration might impede preceding cortical abnormalities. (Baulac et al., 2014) Thus far, *FIG4* mutations can originate into three different autosomal recessive diseases: CMT4J, YVS (Chow et al., 2007; Nicholson et al., 2011) and a multisystem congenital disorder affecting the nervous and musculoskeletal systems, familial epilepsy syndrome with cerebral polymicrogyria (Baulac et al., 2014) CMT4J results from a null *FIG4* mutation in one allele, whilst the other allele carries a hylomorphic missense mutation (I41T or L17P) (Chow et al., 2007, 2009; Nicholson et al., 2011) The I41T mutation has been analysed in mice along with its functional consequences and it is

believed to cause neurodegeneration by destabilizing the Fig4 protein (Ikonomov et al., 2010; Lenk et al., 2011) Fig4 mouse studies suggest that both neurons and glia are required for neuronal survival and function (C. J. Ferguson et al., 2012; Vaccari et al., 2014)

2.5 Objectives

The main goal of the present project was to explore the role of Fig4 in the membrane trafficking and neurodegeneration in CMT4J and other associated neuropathies.

Specifically, the aim of this thesis was to understand the role of Fig4 in regulating the endosomal pathway in order to elucidate the pathomechanisms of these neurological disorders. Moreover, these analyses would also contribute to a better comprehension of phosphoinositides as regulators of membrane trafficking. The specific objectives were:

- To analyse the role of Fig4 in the endo-lysosome system
- To study the impact of the loss of Fig4 activity on the cell viability.

Chapter 3

3. Methods and materials

3.1 Cellular model

HeLa cells were used as a cellular model obtained in CEINGE cell bank and previously present and transfected in the laboratory. In particular, stably Fig4-silenced HeLa cells (Fig4i) were used, by transfecting specific short hairpin RNA. As control, a pool of cells transfected with a short hairpin RNA were used against a random GFP sequence (Ctl). After selection with puromycin and collection of different pools and clones, the efficiency of knockdown was assessed by western blotting.

3.2 Cell Cultures

HeLa cells were maintained in RPMI-1640 medium purchased to Euroclone. The medium was composed by Glycine 10 mg/l, L-Arginine 200 mg/l, L-Asparagine + H_2O 50 mg/l, L-Cystine Dihydrochloride 65.2 mg/l, L-Glutamic acid 20 mg/l, L-Histidine 15 mg/l, L-Hydroxy-L-proline 20 mg/l, L-Isoleucine 50 mg/l, L-Leucine 50 mg/,l L-Lysine + HCl 40 mg/l, L-Methionine15 mg/l, L-Phenylalanine 15 mg/l, L-Proline 20 mg/l, L-Serine 30 mg/l, L-Threonine 20 mg/l, L-Tryptophan 5 mg/l, L-Tyrosine disodium salt dihydrate 28,8 mg/l, L-Valine 20mg/l, Calcium Nitrate Tetrahydrate 100 mg/l, Magnesium sulfate anhydrous 48,8 mg/l, Potassium chloride 400 mg/l, Sodium bicarbonate 2000 mg/l, Sodium chloride 6000 mg/l, Sodium phosphate dibasic anhydrous 2000 mg/l, Choline chloride 3 mg/l, p-Amino Benzoic Acid 1 mg/l, D-Biotin 0.2 mg/l, D-Ca pantothenate 0.25 mg/l, Folic acid 1 mg/l, Myo-inositol 35 mg/l, Nicotinamide 1 mg/l, D-Pantothenic acid 0,25 mg/l, Pyridoxine + HCl 1 mg/l, Riboflavin 0.2 mg/l, Thiamine + HCl 1 mg/l, Vitamin B12 0.005 mg/l, D-Glucose 2000 mg/l, L-Glutathione reduced 1 mg/l, Phenol red 5,3 mg/l. The medium was prepared according to the supplier instructions and mixed with 10% Fetal bovine serum (FBS), 2mM L-glutamine and puromycin (0.6 μg/ml) under incubation at 37º C and in a saturated humidity atmosphere containing 95% air and 5% CO_2. Cells were usually grown on plastic dishes specific for cell cultures and the complete medium is changed every two/three days to provide fresh nutrients for survival and growth.

Cells in culture were routinely observed under a phase contrast microscope (Leica Microsystems) and when confluency was reached, were detached from the plate by using 0.3% trypsin in Phosphate-buffered saline (PBS) pH 7.3 (KCl 13.7 mM, KH_2PO_4 1.47 mM, NaCl 137 mM, Na_2HPO_4 $7H_2O$ 8.06 mM) with the addition of 0.1% glucose and Egtazic acid (EGTA) 2mM, and seeded into new plates. All procedures were carried out in absolute sterility using sterile material and operating under laminar flow hood.

3.3 Growth Curve Assays

Growth curve shows the change in the number of cells in culture over time. Typical curve shows three phases: Lag phase, Log phase and plateau phase.

The assay was carried out by seeding 400,000 cells in 60mm plates. Towards observing the cells, the present culture medium is aspirated under a hood and two quick washes in PBS (NaCl 0.14 M, KCl 0.014 M, Na_2HPO_4 0.008M, KH_2PO_4 0.00147M) are carried out, followed by trypsinization in 500 µl of Trypsin in order to detach the cells in the dish. The cells are then incubated at 37ºC for four to five minutes. Once the cells are detached, they are recovered into a 15ml tube containing culture medium and well suspended through "pipetting" several times up and down. Lastly 100 µl of cell suspension are put into a Neubauer chamber (conversion factor = 10^4) and counted. The cells were counted throughout a period of four days, with medium change every day.

3.4 Fluorescence Assays

For immunofluorescence assays, cells lines were grown on glass coverslips. Cells were washed with PBS, fixed with 4% paraformaldehyde and quenched with 50 mM NH_4Cl. Cells were permeabilized with TX-100 0.2% in PBS, then incubated for 40 min in PBS containing BSA 0.2% and FBS 2%, both used to reduce unspecific antibody binding. Primary antibodies were detected with Alexa Fluor 546 (Invitrogen) conjugated secondary antibodies. After antibodies hybridization, cells were washed using a solution PBS/BSA 0.2/FBS 2%. Finally, coverslips were mounted in slide using PBS/Glycerol (1:1) as mounting medium.

For Lysotracker probes, cells were incubated with the dye LysoTracker® Red DND-99 (ThermoFisher Scientific) (1:1000) for 1 h in complete medium before fixing.

Images were collected using a Zeiss Laser Scanning Confocal Microscope (LSM 510) equipped with a PlanApo 63X oil-immersion (NA 1.4) objective lens. The same settings (80% laser power, 800 detector gain) were used for acquisition.

3.5 Western Blot Assays

Cells were grown on 100 mm petri dishes for three days and lysed with NP40 buffer (Tris pH7.5 20 mM, NaCl 120 mM, NP40 2%) containing 15 μg/ml of protease inhibitor (Antipain, Pepstatin and Leupeptin all from Sigma). Protein extracts were separated by SDS-PAGE (Sodium Dodecyl Sulphate-PolyAcrylamide Gel Electrophoresis), using 10% of acrylamide or 12% when analysing lower molecular mass proteins (e.g., RAB7) and transferred onto Polyvinylidene difluoride (PVDF) membranes. Then, membranes were hybridized with specific primary antibodies (Table 1) that were detected with HRP-conjugated secondary antibodies, visualized with the Pierce ECL Western blotting substrate (Thermo Scientific), according to the manufacture provided protocol.

The several steps of experimental procedure are described:

3.5.1 Cell extracts

Cell extracts were carried out cold on ice to avoid processes of decomposition. Cells seeded on 100 mm diameter cell culture dishes were washed with cold PBS and then mechanically removed using a scraper, collected and centrifuged for 4 minutes at 1000 g (eppendorf centrifuge 5417) in order to sediment the cells. Then, cells were lysed using NP40 buffer, incubating for 30 minutes on ice. After that, the lysates were centrifuged for 30 minutes at 13000 rpm at 4 ºC in the eppendorf 5417R centrifuge. Nuclei and cell debris sediment at the bottom of the tube, while proteins are found in the supernatant.

3.5.2 Bradford assay

To determine the protein concentration of cell lysates, the Bradford method was used. This is a colorimetric method that takes advantage of the affinity of Comassie brilliant blue G250 for arginine, tryptophan, histidine and phenylalanine residues, leading to the production of blue colour measured in the spectrophotometer at 595 nm. In particular for this analysis, the Bradford kit manufactured by Biorad (Protein Assay Reagent, Biorad Laboratories Inc.) was used according to the indications of the manufacturer (dilution 1:5 with distilled water).

In order to determine protein concentration, it was necessary to make a standard curve by measuring the absorbance of solutions with known protein concentration (shown in the Supplementary results). For each dosage, a standard curve was obtained using 1, 2 and 4 μg/ml of albumin. The resulting curve allowed extrapolating the concentration of protein in the obtained lysates on the basis of Lambert-Beer law which established a direct proportionality between absorbance and protein concentration.

3.5.3 SDS-PAGE

The gels were prepared using a 30% mixture of acrylamide and N,N'-methylenebis-acrylamide with a 37.5:1 mass ratio respectively.

SDS-PAGE was carried out by using a Mini Protean III (Biorad) equipment. The samples were suspended in Laemmli 2X buffer (Tris 1M pH 6.8, SDS 10%, glycerol 20%, bromine phenol 0.05% and β-mercaptoethanol 10%), in a 1:1 ratio of Laemmli 2X and protein lysate. Before loading the gel, the samples were boiled at 100 ºC for 5 minutes for protein denaturation and, then, centrifuged at 17,000g in one bench-top spin (eppendorf centrifuge 5417) for 2 min.

The electrophoresis chamber was filled with the running buffer (Tris 25 mM, Glycine 190 mM, SDS 0.1% in water).

3.5.4 Western blotting

Once separated, the proteins were transferred into polyvinylidene fluoride (PVDF) membranes. The transfer was carried out at 4°C in transfer buffer (Tris 25 mM, Glycine 190 mM, Methanol 20%) for 3h or overnight by applying a constant amperage of 350 mA or 150 mA, respectively (BioRad). Then, the membrane was incubated for 2h at room temperature in a “blocking solution” containing 5% dry milk in TBST solution (20 mM Tris, 150 mM NaCl, 0.1% Tween 20)

Antibody hybridization was performed in 2.5% milk dissolved in TBST, and the time of incubation was 1 or 2 hours at room temperature or overnight, (depending on the affinity of each antibody); four ten-minute washings after primary and secondary (HRP-conjugated) antibodies were carried out using the TBST solution and a 3D rocking shaker. Finally, samples were detected through chemiluminescence.

Table 1 - List of studied proteins and primary antibodies used for hybridization

Protein	Molecular weight (kDa)	Primary antibody	Antibody type
EEA1	170	Anti-EEA1 (Rabbit)	Polyclonal
LAMP-1	110's	Anti-LAMP-1 (Mouse)	Monoclonal
Cathepsin D	33, 46, 52	Anti-Cathepsin (Rabbit)	Polyclonal
α-Tubulin	50	Anti-α-Tubulin (Mouse)	Monoclonal
GAPDH	37	Anti-GAPDH (Mouse)	Monoclonal
RAB7	23/24	Anti-RAB7 (Rabbit)	Polyclonal

3.6 Densitometric Analysis

Films were acquired by the computer as tiff format images thanks to the use of a scanner set in "greyscale" mode, at 300 dpi (Films presented in chapter 4 and Annexes). The densitometric analysis was carried out through the use of ImageJ software, which provides the density values of the bands in terms of area and pixel intensity. By placing the command "Analyze Measure " Image J provides information concerning the area of the bands and grey levels. The numerical values obtained are directly proportional to the intensity of each band. In particular, we have drawn a region of interest of rectangular shape around the band and the same area was measured for the bands of the gel.

Chapter 4

4. Results and discussion

4.1 HeLa cells' transfections

In order to analyse the role of Fig4 on the endosomal pathway, the effects of the knockdown of its expression in non-neuronal and neuronal cells, were investigated in the research group where the thesis was developed. Since Fig4 is ubiquitously expressed as aforementioned, a non-neuronal HeLa cell line was used due to its easiness to handle and being transfectable with good efficiency.

As shown in Figure 6, pools and clones (derived from a single cell) displayed a range of silencing from 30 to 80% and those with a reduction of about 40-45% were used for further experiments.

Moreover, by western blot analysis the silencing was verified to be stable and was maintained in the cells in culture until at least the fourth passage (later ones were not tested) the experiments were always performed no later than the third passage in culture.

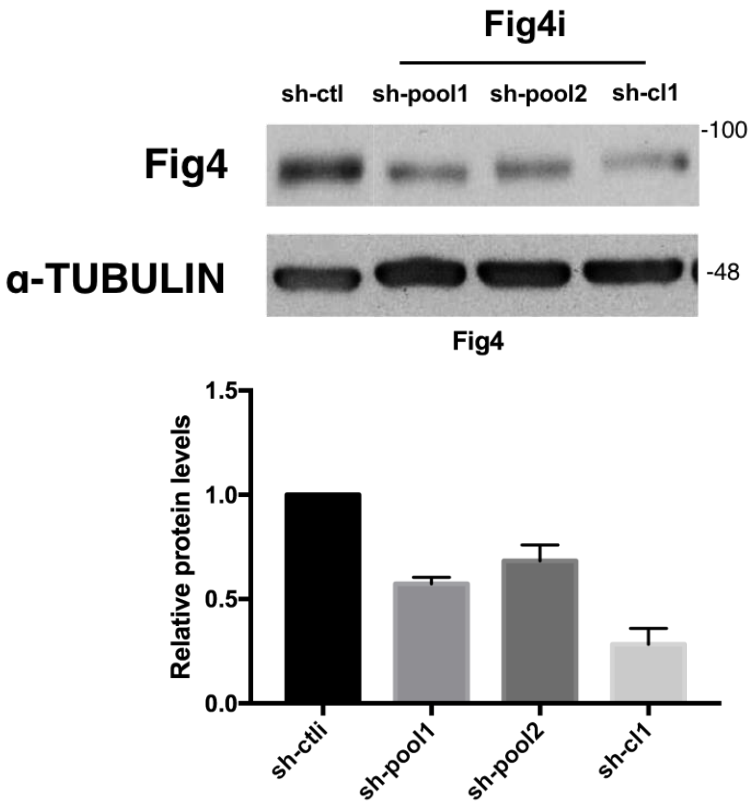

Figure 6 - Fig4 expression is knockdown in Hela cells. HeLa cells stably transfected with anti-Fig4 and scramble shRNAs were immunoblotted with an anti-Fig4 antibody. α-tubulin was used as loading control. Molecular weights of proteins are indicated

4.2 Analysis of LAMP-1 in Ctli and Fig4i HeLa cells

As aforementioned some studies have reported that fibroblasts of CMT4J patients and pale tremor (plt) mice (model organism of the disease) display enlarged LAMP1/2 positive vacuoles (Katona et al., 2011; Zhang et al., 2008; Y. Zhang et al., 2007), suggesting that the deficiency of Fig4 activity may lead to the dysfunction of these compartments.

To test this hypothesis, the morphology and dynamics of the lysosomal compartments in either Fig4-silenced cells (Fig4i) or scrambled RNA transfected control cells (Ctli) were analysed by immunofluorescence assays. Cells were seeded on glass coverslips and grown for 3 days. Lysosomes were labelled with Lysotracker dye Red DND-99, a cell permeable dye that stains acidic compartments in live cells, or using a specific antibody anti-LAMP1, a membrane anchored protein resident in these organelles (Figure 7). Upon observing Figure 7 the lysosomal compartments appear dyed in red in both Ctli and Fig4i cells. Regarding Lamp-1 fluorescence assay, the Fig4i lysosomal compartments appear enlarged and more numerous in comparison with Ctli ones. The graphic evidencing the fluorescence intensity corroborates with this result since Fig4i cells appear to have a higher fluorescence intensity when compared to Ctli, evidencing a higher LAMP-1 concentration .

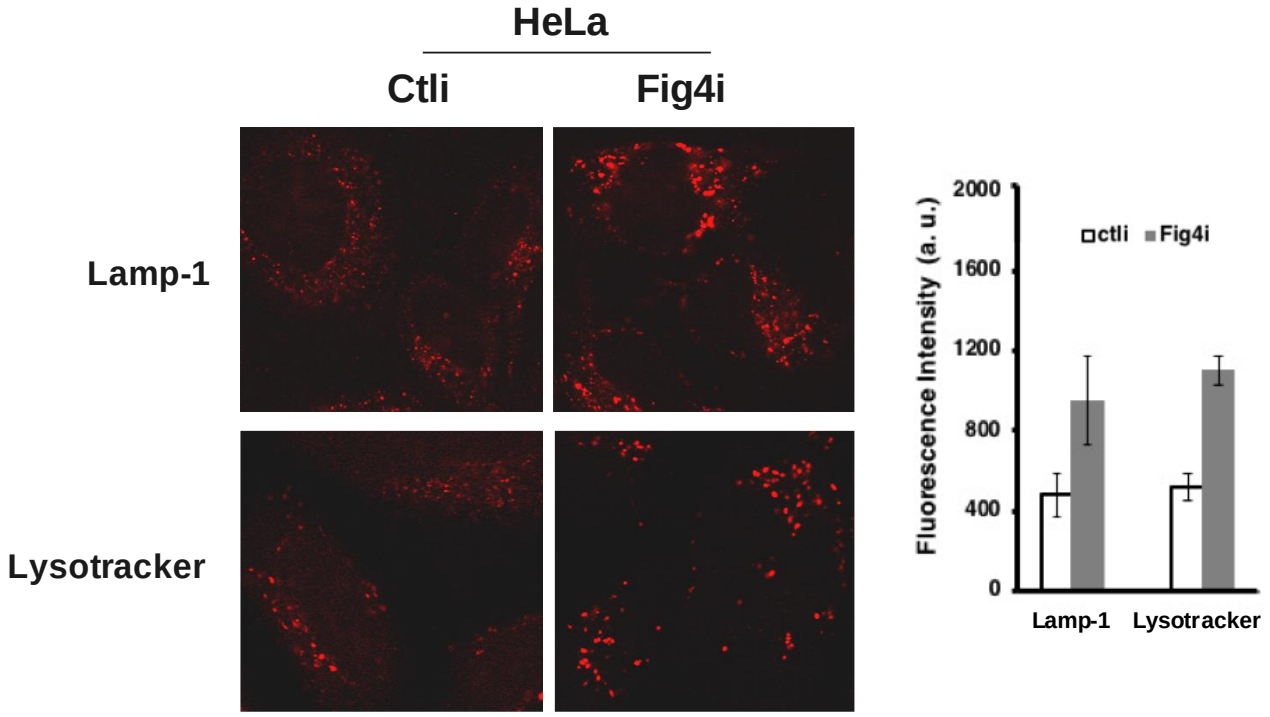

Figure 7 - The loss of Fig4 leads to an enlargement of lysosomal compartments. Ctli and Fig4i cells were subjected to immunofluorescence assay by using anti-Lamp1 antibody (left panel). Alternatively, cells were incubated with Lysotracker for 1h at 37 °C and then fixed. Images were acquired by confocal microscopy by using the same settings (laser power, detector gain). Quantification of fluorescence intensity is shown in the graph

In what concerns Lysotracker, the same conclusion obtained in LAMP-1 assay is presented. Fig4i cells are shown with bigger and more numerous lysosomal stained compartments appearing as large dots, as well as presenting a stronger fluorescent signal in comparison with Ctli. These results are expected according to the already LAMP1/2 vacuoles observed in patients with CMT4J or pale tremor mice, which present Fig4 mutations and deficiency. Thus, it can be concluded that lysosomal compartments are drastically altered in Fig4 knockdown cells, observed both with the Lysotracker dye or with LAMP-1 antibody, with lysosomes appearing increased in number and as large dots with strong fluorescent signal (Figure 7), indicating an enlargement of lysosomes.

Towards understanding if lysosomal compartment dynamics are also altered, western blot analysis on LAMP-1 of cells lysate extracted with NP40 detergent of Fig4i cells and Ctli cells was made. The results obtained from the western blot are presented in Figure 8 and in Annex 2. Figure 8 shows that LAMP-1 is evidenced at a lower expression

in the Ctli band and a gradual higher expression with thicker and darker bands in Fig4 silenced bands, pool1 and Clone1 band accordingly. Through these results, it can be concluded that, the higher the degree of Fig4 silencing, the higher the amount of LAMP-1 protein expression levels. In order to ensure that differences observed were not due to protein loading, blots were then reprobed and analysed for α-tubulin levels where normalization can be observed since all the samples show the same protein expression levels with similar bands in thickness and tonality, concluding that the western blot went according to the expectations in terms of protein loaded among the bands.

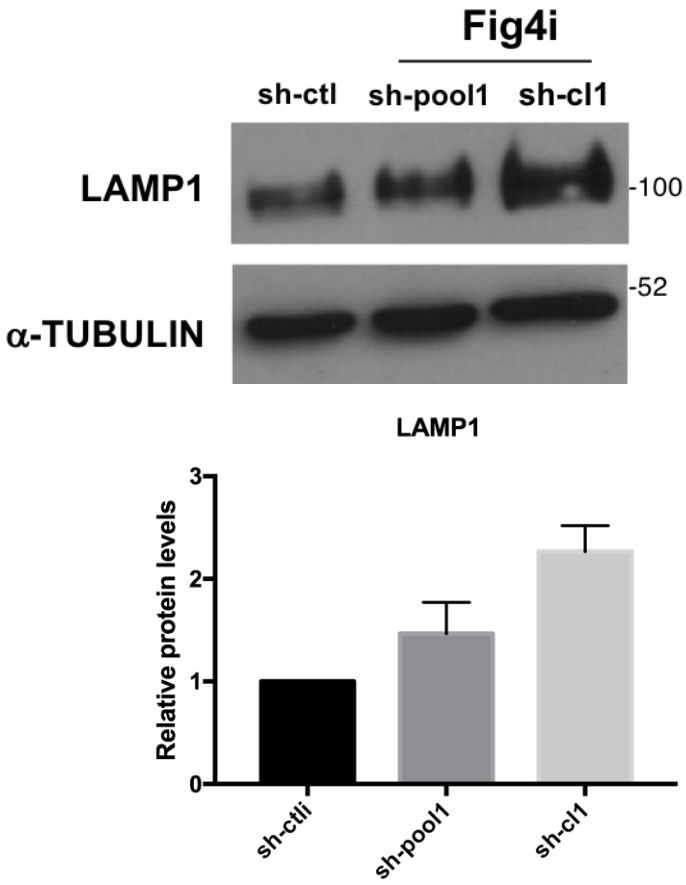

Figure 8 - Lamp1 levels are increased upon Fig4 loss. Ctli and Fig4i cells were immunoblotted with an anti-Lamp1 antibody; α-tubulin was used as loading control. Molecular weights of proteins are indicated. Relative quantification of bands is shown in the graph

The histogram, also presented at Figure 8, containing the different LAMP-1 quantifications, has been made, confirming what was analysed in the previous western blots. Fig4i Clone1 band, besides showing the highest Fig4i of all the cells, it also demonstrates a higher LAMP-1 quantification, a lysosomal marker, followed by pool1 and Ctli.

Altogether, the results presented from the immunofluorescence assays and the western blots show increased evidence that Fig4 knockdown could result in a disruption of lysosomal organelles dynamics and homeostasis in the endocytic pathway, and that Fig4 presents a role in managing the lysosomes. These results are expected since they are in agreement with observations made in the fibroblasts of plt mice and patients (Chow et al., 2007; Zhang et al., 2008).

It is worth noting that the increased LAMP-1 levels correlate with the degree of silencing, further corroborating the importance of this protein in regulating these organelles.

4.3 Western blot of endosomal markers EEA1 and RAB7 in Fig4i cells

Live-cell imaging reveals the endolysosomal system as a complex and highly dynamic network of interacting compartments. Thus, towards understanding if whether the endosomal compartments might be dependent on Fig4 activity, the expression levels of endosomal proteins: EEA1 (Early Endosomal Antigen 1) and RAB7, which are specific markers of early and late endosomes respectively, were assessed (Figure 9 and 10). Cells were lysed with buffer containing the non-ionic detergent NP40 and protein samples were separated on SDS-PAGE (as described in detail in methods).

Observing the film from EEA1 analysis on Figure 9, reminiscent of LAMP-1, a higher expression of EEA1 is noticeable from Clone1 Fig4 silenced band, in comparison with Pool that contains a lower Fig4i and Ctli with no Fig4i, which could represent an altered homeostasis and disruption in early endosomes. Western blot analyses showed higher levels of EEA1 in Fig4i cells at dose-dependent manner (Figure 9): the most silenced clone displays highest levels of EEA1. The histogram presented shows the relative protein quantification levels of all the western blots made to analyse EEA1. The representation of these results affirms that the higher the degree of Fig4 silencing, the higher the amount of EEA1 expression, showing an alteration in the early endosome dynamics in comparison with non-Fig4 silenced cells.

In order to verify that the differences observed weren't derived from protein loading, blots were analysed for GAPDH relative levels. Inspecting the GAPDH bands and analysing their relative quantification in imageJ, normalization can be concluded. This result was not expected since there was no evidence in the literature regarding Fig4 silencing leading to early endosome alteration and EEA1 was not present in vacuoles formed. (Katona et al., 2011; Zhang et al., 2008). This novel evidence may highlight the role of Fig4 in controlling the whole endo-lysosome axis, and further investigation may help elucidate these results and how related pathomechanisms may intervene in Fig4-related diseases.

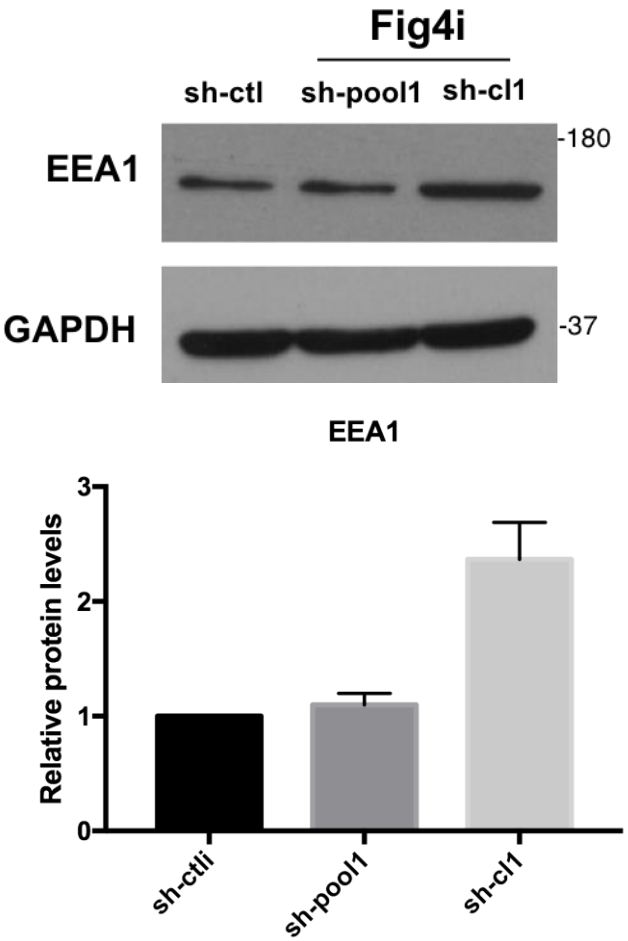

Figure 9 - EEA1 levels are increased upon Fig4 loss. Ctli and Fig4i cells were immunoblotted with an anti-EEA1 antibody; GAPDH was used as loading control. Molecular weights of proteins are indicated. Relative quantification of bands is shown in the graph

In a further analysis, to understand how late endosomes are influenced by Fig4 knockdown, RAB7 a marker of late endosomes, was analysed by western blot. Figure 10 shows the results of this experiment, where once again three cultures were studied, Ctli and Fig4i cells, Pool1 and Clone1. Concerning control interfered band, it can be visualized a more faded and smaller band compared to the remaining ones evidenced. Pool Fig4i band is the intermediate band in terms of protein expression with higher quantity of RAB7 compared to Ctli and lower than the one presented by Fig4i Clone1. Clone1, the band with the highest Fig4 silencing is the band with also the highest RAB7 protein expression of the film. To ensure that differences observed were not due to protein loading, blots were then reprobed and analysed GAPDH levels. Examining Figure 10, the bands obtained from this experiment seem to present the same intensity as well as the same size, therefore being possible to affirm linearization, and validate the results from the protein quantification

analysed previously.

The present histogram of the western blot made for RAB7 analysis represents a clear RAB7 increase, as mentioned in the film obtained from the western blot, in Fig4i cultures, with the highest quantification being present in Fig4 silenced Clone1 band. Thus, the higher Fig4 silencing corresponds to a higher amount of RAB7 quantification. This data may indicate an alteration in late endosomes dynamics in the endocytic pathway, evidenced in Fig4 knockdown cells, since RAB7 is presented as a late endosome marker.

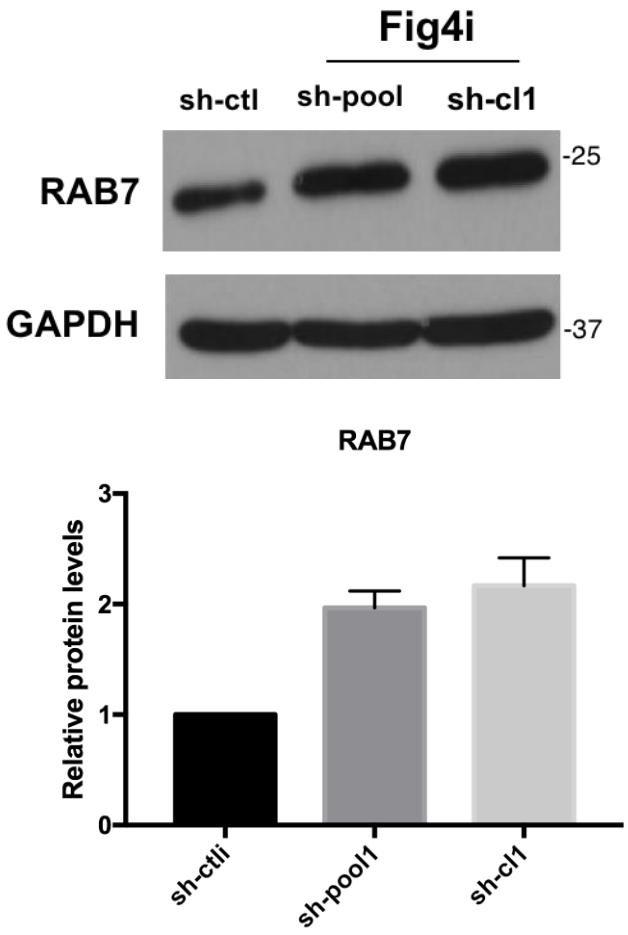

Figure 10 - Rab7 levels are increased upon Fig4 loss. Ctli and Fig4i cells were immunoblotted with an anti-Rab7 antibody; GAPDH was used as loading control. Molecular weights of proteins are indicated. Relative quantification of bands is shown in the graph

These results are expected since it is indicated in the literature that RAB7 is highly presented in late endosomes and in LAMP-1 positive structures.(Lebrand et al., 2002; Vonderheit & Helenius, 2005) Thus, from the increase of LAMP-1 previously observed in Figure 7 and 8, it is expected to observe a higher RAB7 concentration in Fig4i cells in comparison to Ctli.

In agreement with these data, it was observed, in the research group where the present thesis was developed, a strong alteration of the structure of endosomal compartments assessed by immunofluorescence assays.

Overall, these data indicate that the loss of Fig4 affects the homeostasis and dynamics of the endo-lysosomal axis. Thus, there is a relevant importance in investigating whether and how the loss of Fig4 affects the functions of these compartments by evaluating the trafficking pathways regulated by endosomal compartments and the degradation activity of lysosomes.

4.4 Examination of the proliferation rate on Fig4i cells

From the data already obtained, it is shown that the loss of Fig4 clearly alters the homeostasis of endo-lysosomal system. Thus, a research in the impact of this alteration on the cell physiology was done. To answer this question and for a better understanding of the pathophysiological role of Fig4, it was assessed whether and how the levels of expression of Fig4 impaired cell proliferation and metabolism.

To assess the proliferation rate, the growth of control and Fig4 silenced cells over time was monitored. To this aim, 400,000 cells were seeded in 60 mm diameter plates and the cells were counted every 24 hours. Specifically, for each timepoint cells were detached from the dish using a solution containing trypsin (a proteolytic enzyme that cleaves proteins in correspondence of basic amino acids) and the cells were counted using a Neubauer's cell-counting chamber.

Figure 16 presented in the Annex 3, contains the data obtained and processed from counting the plated cells from different interfered cells, Ctli and Fig4 silenced cells, Pool and Clone1. The first of two growth curves were made for Ctli cultures and Fig4 silenced HeLa cultures, Pool and Clone1 (Cl1), for a period of four days. A major growth from control interfered cells can be observed in comparison with Fig4i cells, Pool and Cl1 throughout the whole four days, whereas Clone1 is the culture with the least number of cells, until the last day where it surpasses Pool with an exponential growth. This growth and change of behaviour may be explained, perhaps due to a miscounting, since the remaining cultures' growth remained stable throughout the final day. Taking in consideration the aspect of the curve, it can be observed that all cultures begin at approximately 200,000 cells with Fig4 silenced Pool culture a slightly over this number. Across the first day, there is a small growth regarding both silenced Fig4 cultures and an even bigger growth from controlled interfered cells, representing the Lag phase of a standard cell culture growth, where cells start getting accustomed to the involving environment. In the following days, the cultures start showing an increased growth in comparison with the previous day, showing indices of the Log phase, representing an exponential growth phase. The cultures maintain their growth until the last day, evidencing a slight decrease in Pools' culture slope, representing cell growth, whereas Clone1 culture, as mentioned before, shows an increased growth, almost surpassing Ctli culture that

maintains its growth. The graphic allows the conclusion that the higher the Fig4 silencing is, the less cells are prominent to grow, despite Clone1 culture showing an abnormal and unexpected behaviour from the third to the fourth day, evidencing a substantial growth in comparison with the remaining cultures. A miscounting might explain these results since there is no apparent reason for the culture behaviour. No stationary phase seems to be present in either of cultures throughout the growth curve period.

Thus, below a new counting has been made presented at Figure 11 to obtain consistency and better results than the ones obtained before, containing a growth curve with the following number of live cells counted in function of time in hours, taken in consideration once again, the different cell type

At first glance, the graphic already shows better consistency and coherence then the one from Figure 16, evidencing a more representative and trustable behaviour. An overall

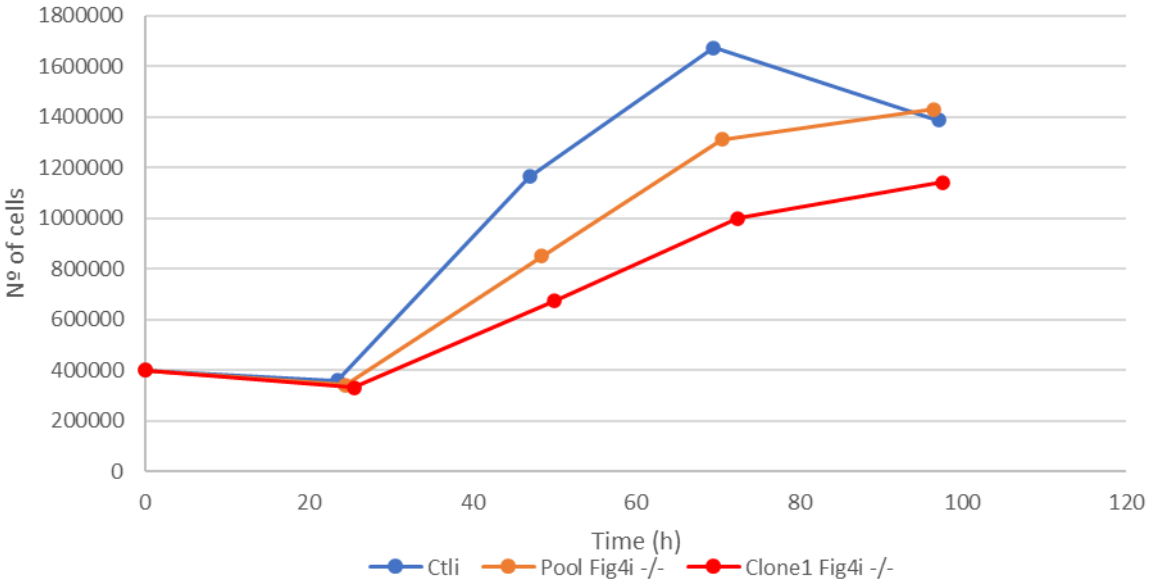

Figure 11 - The loss of Fig4 affects the cell growth. Ctli and Fig4i cells were seeded on 60 mm diameter dishes; the cell growth was monitored counting every 24 hours. Representative growth curves are shown in the graphic

examination of the different slopes of the curves concludes that Ctli cells have an increase number of cells in comparison with Fig4 silenced cells, Pool and Clone1, throughout the whole incubation period, excluding the last day where there is a major decrease in the number of cells, showing a lower number than Fig4i Pool culture. Fig4i Clone1 also shows evidence of being the culture with less growth in comparison with Pool and Ctli. A correlation between the degree of Fig4 silencing and the number of cells is likely concluded, since the number of cells is lower, the higher the degree of Fig4 silencing is,

where Clone1 shows the highest Fig4 silencing followed by Pool culture and Ctli with no Fig4 silencing. Examining the growth curve, on the first day from the moment the cells are first plated, all cultures contain a total of 400,000 cells, decreasing in number throughout the first day, representing the Lag phase of the incubation where the cells are adjusting to the environment they are on, with all cultures showing approximately the same decrease in cell numbers. From this point forward, cells start entering the exponential phase, where their growth increases exponentially until the third day. Despite all cultures increasing in number of cells, there is a difference in percentage of growth, where Control interfered cells grow at a higher rate, followed by Pool and Clone1 Fig4i cultures respectively. The continued growth lasts until the third day, where from that point forward, the control interfered culture decreases in cell number. This may be explained due to the high number of cells present in the dish and achieved confluency, demonstrating contact inhibition present in the dish, since the cells do not have any more space to grow, the number of cells is decreased. On the last day, Fig4 silenced cultures, Pool and Clone1, contrarily to controlled interfered, continue to develop in numbers. This growth curve exposes the possibility that, the higher the degree of Fig4 silencing in cultures, the less cells are prominent to grow, where Clone1 with the higher Fig4 silencing has the lowest number of cells followed by Pool and Control with no interference which evidences more resilient and durable cells.

This examination concludes that loss of Fig4 affects the cellular proliferation. Moreover, these data also suggest that the alterations of endo-lysosomal pathway influence cell viability, despite not being evidenced how.

Chapter 5

5. Conclusion

Mutations in the inositol phosphatase Fig4 were firstly associated with Charcot-Marie-Tooth 4J (CMT4J) neuropathy. Later, frameshift and other missense mutations have been reported to be responsible of Yunis-Varon syndrome and familial epilepsy with polymicrogyria extending the spectrum of phenotypes associated with Fig4 mutations. Fig4 is ubiquitous and dephosphorylates the endolysosome-enriched $PI(3,5)P_2$ to generate PI(3)P. Although it is not yet well understood how phosphoinositides act, it is clear that these lipids play an important role in regulating membrane trafficking. Therefore, it is essential that their levels are finely controlled.

Interestingly, *FIG4* mutations, including those associated with CMT4J, do not alter its catalytic activity. Enlarged LAMP-2 positive vacuoles with watery appearance or filled with electron dense material (depending on cell type) are found in neurons, muscle, and cartilage of Fig4 null mice, suggesting a dysfunction of these compartments. However, the pathogenic mechanism(s) still remain elusive, as well as its role in regulating these organelles.

In agreement with observations in plt mice and CMT4J patient fibroblasts (Chow et al., 2007; Zhang et al., 2008), it was observed that in Fig4-silenced cells, lysosomes and late endosomes appear enlarged and more abundant. Moreover, also late endosomes appear as large dots upon Fig4 silencing, indicating that Fig4 is crucial for the homeostasis of these organelles. On the other hand, considering that $PI(3,5)P_2$ is enriched in these compartments, these data also indicate that proper concentration of this PI is essential for the regulation of these organelles. Strikingly, in this experiment there is evidence that the loss of Fig4 also affects early endosomes. Overall, the loss of Fig4 activity leads to drastic changes in the endo-lysosomal system according to the data obtained. Preliminary data of the research group where the thesis was developed, show that defects of endosomal trafficking exist in Fig4 knockdown cells.

The endo-lysosomal system, which is a crossroad of distinct intracellular pathways, has emerged and is still emerging as key player in various neurological disorders. Hence, the results presented further strengthen the existence of a functional link between endosomal trafficking and neurological disorders.

The impaired growth of Fig4 knockdown HeLa cells further indicates that the endo-lysosomal pathway is critical for cellular survival, evidenced on the performed growth curve.

5.1 Future Work

Further studies in neuronal cells will be important to understand the role of Fig4 in neurons and the pathogenesis of Fig4-associated diseases.

In order to better understand how Fig4 controls the endocytic compartments, it will be important to evaluate the impact of Fig4 loss on the functions of these organelles. The next challenge could also be to understand how the dysfunction of endosomal compartments may lead to neurodegeneration. The hypothesis that the dysfunction of endocytic compartments and endosomal trafficking correlates with the alteration of neuronal plasticity or with the loss of neuronal viability is plausible.

It is likely that the impairment of the trafficking of specific neural proteins (e.g., growth factors and neurotransmitter receptors, proteins implicated in neuritogenesis) may be critical for the development of diseases. This would also explain the high sensitivity of neurons with respect to other cell types.

It could also be important to evaluate and compare the metabolic state of control and Fig4-silenced cells by using, for example, MTT assays. To unravel the link among Fig4 activity, endo-lysosomal pathway and cell survival and function, will be the next challenge to shed light on pathogenic mechanisms of Fig4-associated diseases.

Chapter 6

6. Bibliography

Balla, T. (2005). Inositol-lipid binding motifs: Signal integrators through protein-lipid and protein-protein interactions. *Journal of Cell Science*, *118*(10), 2093–2104. https://doi.org/10.1242/jcs.02387

Banta, L. M., Vida, T. A., Herman, P. K., & Emr, S. D. (1990). Characterization of yeast Vps33p, a protein required for vacuolar protein sorting and vacuole biogenesis. *Molecular and Cellular Biology*, *10*(9), 4638–4649. https://doi.org/10.1128/mcb.10.9.4638

Baulac, S., Lenk, G. M., Dufresnois, B., Bencheikh, B. O. A., Couarch, P., Renard, J., Larson, P. A., Ferguson, C. J., Noé, E., Poirier, K., Hubans, C., Ferreira, S., Guerrini, R., Ouazzani, R., El Hachimi, K. H., Meisler, M. H., & Leguern, E. (2014). Role of the phosphoinositide phosphatase FIG4 gene in familial epilepsy with polymicrogyria. *Neurology*, *82*(12), 1068–1075. https://doi.org/10.1212/WNL.0000000000000241

Berridge, M. J., & Irvine, R. F. (1989). Inositol phosphates and cell signalling. *Nature*, *341*(6239), 197–205. https://doi.org/10.1038/341197a0

Béthune, J., Wieland, F., & Moelleken, J. (2006). COPI-mediated transport. *Journal of Membrane Biology*, *211*(2), 65–79. https://doi.org/10.1007/s00232-006-0859-7

Botelho, R. (2008). Assembly of a Fab1 Phosphoinositide Kinase Signaling Complex Requires the Fig4 Phosphoinositide Phosphatase. *Molecular Biology of the Cell*, *19*(October). https://doi.org/10.1091/mbc.E08

Campeau, P. M., Lenk, G. M., Lu, J. T., Bae, Y., Burrage, L., Turnpenny, P., Román Corona-Rivera, J., Morandi, L., Mora, M., Reutter, H., Vulto-Van Silfhout, A. T., Faivre, L., Haan, E., Gibbs, R. A., Meisler, M. H., & Lee, B. H. (2013). Yunis-Varón syndrome is caused by mutations in FIG4, encoding a phosphoinositide phosphatase. *American Journal of Human Genetics*, *92*(5), 781–791. https://doi.org/10.1016/j.ajhg.2013.03.020

Chow, C. Y., Landers, J. E., Bergren, S. K., Sapp, P. C., Grant, A. E., Jones, J. M., Everett, L., Lenk, G. M., McKenna-Yasek, D. M., Weisman, L. S., Figlewicz, D., Brown, R. H., & Meisler, M. H. (2009). Deleterious Variants of FIG4, a Phosphoinositide Phosphatase, in Patients with ALS. *American Journal of Human Genetics*, *84*(1), 85–88. https://doi.org/10.1016/j.ajhg.2008.12.010

Chow, C. Y., Zhang, Y., Dowling, J. J., Jin, N., Adamska, M., Shiga, K., Szigeti, K., Shy, M. E., Li, J., Zhang, X., Lupski, J. R., Weisman, L. S., & Meisler, M. H. (2007). Mutation of FIG4 causes neurodegeneration in the pale tremor mouse and patients with CMT4J. *Nature*, *448*(7149), 68–72. https://doi.org/10.1038/nature05876

De Matteis, M. A. (2011). Mendelian disorders of membrane trafficking. *New England Journal of Medicine*, *365*(21), 2038–2039. https://doi.org/10.1056/NEJMc1111685

De Matteis, M. A., & Godi, A. (2004). PI-loting membrane traffic. *Nature Cell Biology*, *6*(6), 487–492. https://doi.org/10.1038/ncb0604-487

De Matteis, M. A., & Luini, A. (2008). Exiting the Golgi complex. *Nature Reviews Molecular Cell Biology*, *9*(4), 273–284. https://doi.org/10.1038/nrm2378

Di Paolo, G., & De Camilli, P. (2006). Phosphoinositides in cell regulation and membrane dynamics. In *Nature* (Vol. 443, Issue 7112). https://doi.org/10.1038/nature05185

Doherty, G. J., & McMahon, H. T. (2009). Mechanisms of Endocytosis. *Annual Review of Biochemistry*, *78*(1), 857–902. https://doi.org/10.1146/annurev.biochem.78.081307.110540

Dove, S. K., Cooke, F. T., Douglas, M. R., Sayers, L. G., Parker, P. J., & Michell, R. H. (1997). Osmotic stress activates phosphatidylinositol-3,5-bisphosphate synthesis. *Nature*, *390*(6656), 187–192. https://doi.org/10.1038/36613

Duex, J. E., Nau, J. J., Kauffman, E. J., & Weisman, L. S. (2006). Phosphoinositide 5-phosphatase Fig4p is required for both acute rise and subsequent fall in stress-induced phosphatidylinositol 3,5-bisphosphate levels. *Eukaryotic Cell*, *5*(4), 723–731. https://doi.org/10.1128/EC.5.4.723-731.2006

Efe, J. A., Botelho, R. J., & Emr, S. D. (2005). The Fab1 phosphatidylinositol kinase pathway in the regulation of vacuole morphology. *Current Opinion in Cell Biology*, *17*(4), 402–408. https://doi.org/10.1016/j.ceb.2005.06.002

Ellgaard, L., & Helenius, A. (2003). Quality control in the endoplasmic reticulum. *Nature Reviews Molecular Cell Biology*, *4*(3), 181–191. https://doi.org/10.1038/nrm1052

Erdman, S., Lin, L., Malczynski, M., & Snyder, M. (1998). Pheromone-regulated genes required for yeast mating differentiation. *Journal of Cell Biology*, *140*(3), 461–483. https://doi.org/10.1083/jcb.140.3.461

Falkenburger, B. H., Jensen, J. B., Dickson, E. J., Suh, B. C., & Hille, B. (2010). Phosphoinositides: Lipid regulators of membrane proteins. *Journal of Physiology*,

588(17), 3179–3185. https://doi.org/10.1113/jphysiol.2010.192153

Ferguson, C. J., Lenk, G. M., Jones, J. M., Grant, A. E., Winters, J. J., Dowling, J. J., Giger, R. J., & Meisler, M. H. (2012). Neuronal expression of Fig4 is both necessary and sufficient to prevent spongiform neurodegeneration. *Human Molecular Genetics*, *21*(16), 3525–3534. https://doi.org/10.1093/hmg/dds179

Ferguson, Cole J., Lenk, G. M., & Meisler, M. H. (2009). Defective autophagy in neurons and astrocytes from mice deficient in PI(3,5)P2. *Human Molecular Genetics*, *18*(24), 4868–4878. https://doi.org/10.1093/hmg/ddp460

Ho, C. Y., Alghamdi, T. A., & Botelho, R. J. (2012). Phosphatidylinositol-3,5-bisphosphate: No longer the poor PIP 2. *Traffic*, *13*(1), 1–8. https://doi.org/10.1111/j.1600-0854.2011.01246.x

Hughes, W. E., Cooke, F. T., & Parker, P. J. (2000). Sac phosphatase domain proteins. *Biochemical Journal*, *350*(2), 337–352. https://doi.org/10.1042/0264-6021:3500337

Ikonomov, O. C., Sbrissa, D., Fligger, J., Delvecchio, K., & Shisheva, A. (2010). ArPIKfyve regulates Sac3 protein abundance and turnover disruption of the mechanism by Sac3I41T mutation causing charcot-marie-tooth 4J disorder. *Journal of Biological Chemistry*, *285*(35), 26760–26764. https://doi.org/10.1074/jbc.C110.154658

Ikonomov, O. C., Sbrissa, D., Ijuin, T., Takenawa, T., & Shisheva, A. (2009). Sac3 Is an Insulin-regulated Phosphatidylinositol 3,5-bisphosphate phosphatase. Gain in insulin responsiveness through Sac3 down-regulation in adipocytes. *Journal of Biological Chemistry*, *284*(36), 23961–23971. https://doi.org/10.1074/jbc.M109.025361

Jin, N., Chow, C. Y., Liu, L., Zolov, S. N., Bronson, R., Davisson, M., Petersen, J. L., Zhang, Y., Park, S., Duex, J. E., Goldowitz, D., Meisler, M. H., & Weisman, L. S. (2008). VAC14 nucleates a protein complex essential for the acute interconversion of PI3P and PI(3,5)P2 in yeast and mouse. *EMBO Journal*, *27*(24), 3221–3234. https://doi.org/10.1038/emboj.2008.248

Katona, I., Zhang, X., Bai, Y., Shy, M. E., Guo, J., Yan, Q., Hatfield, J., Kupsky, W. J., & Li, J. (2011). Distinct pathogenic processes between Fig4-deficient motor and sensory neurons. *European Journal of Neuroscience*, *33*(8), 1401–1410. https://doi.org/10.1111/j.1460-9568.2011.07651.x

Krauß, M., & Haucke, V. (2007). Phosphoinositide-metabolizing enzymes at the interface

between membrane traffic and cell signalling. *EMBO Reports*, *8*(3), 241–246. https://doi.org/10.1038/sj.embor.7400919

Kulkarni, M. L., Vani, H. N., Nagendra, K., Mahesh, T. K., Kumar, A., Haneef, S., Mohammed, Z., & Kulkarni, P. M. (2006). Yunis varon syndrome. *Indian Journal of Pediatrics*, *73*(4), 353–355. https://doi.org/10.1007/BF02825832

L. Volpicelli, P. D. C. (2007). Phosphoinositides' link to neurodegeneration. *Nature*, *448*(7151), 313–317. https://doi.org/10.1038/nature05934

Lebrand, C., Corti, M., Goodson, H., Cosson, P., Cavalli, V., Mayran, N., Fauré, J., & Gruenberg, J. (2002). Late endosome motility depends on lipids via the small GTPase Rab7. *EMBO Journal*, *21*(6), 1289–1300. https://doi.org/10.1093/emboj/21.6.1289

Lemmon, M. A. (2003). Phosphoinositide recognition domains. *Traffic*, *4*(4), 201–213. https://doi.org/10.1034/j.1600-0854.2004.00071.x

Lenk, G. M., Ferguson, C. J., Chow, C. Y., Jin, N., Jones, J. M., Grant, A. E., Zolov, S. N., Winters, J. J., Giger, R. J., Dowling, J. J., Weisman, L. S., & Meisler, M. H. (2011). Pathogenic mechanism of the FIG4 mutation responsible for charcot-marie-tooth disease CMT4J. *PLoS Genetics*, *7*(6). https://doi.org/10.1371/journal.pgen.1002104

Lin, W., & Popko, B. (2009). Endoplasmic reticulum stress in disorders of myelinating cells. *Nature Neuroscience*, *12*(4), 379–385. https://doi.org/10.1038/nn.2273

Manford, A., Xia, T., Saxena, A. K., Stefan, C., Hu, F., Emr, S. D., & Mao, Y. (2010). Crystal structure of the yeast Sac1: Implications for its phosphoinositide phosphatase function. *EMBO Journal*, *29*(9), 1489–1498. https://doi.org/10.1038/emboj.2010.57

Martin, T. F. J. (1998). PHOSPHOINOSITIDE LIPIDS AS SIGNALING MOLECULES: Common Themes for Signal Transduction, Cytoskeletal Regulation, and Membrane Trafficking. *Annual Review of Cell and Developmental Biology*, *14*(1), 231–264. https://doi.org/10.1146/annurev.cellbio.14.1.231

Mayinger, P. (2012). Phosphoinositides and vesicular membrane traffic. *Biochimica et Biophysica Acta - Molecular and Cell Biology of Lipids*, *1821*(8), 1104–1113. https://doi.org/10.1016/j.bbalip.2012.01.002

Michell, R. H., Heath, V. L., Lemmon, M. A., & Dove, S. K. (2006). Phosphatidylinositol 3,5-bisphosphate: Metabolism and cellular functions. *Trends in Biochemical Sciences*, *31*(1), 52–63. https://doi.org/10.1016/j.tibs.2005.11.013

Nicholson, G., Lenk, G. M., Reddel, S. W., Grant, A. E., Towne, C. F., Ferguson, C. J.,

Simpson, E., Scheuerle, A., Yasick, M., Hoffman, S., Blouin, R., Brandt, C., Coppola, G., Biesecker, L. G., Batish, S. D., & Meisler, M. H. (2011). Distinctive genetic and clinical features of CMT4J: A severe neuropathy caused by mutations in the PI(3,5)P2 phosphatase FIG4. *Brain*, *134*(7), 1959–1971. https://doi.org/10.1093/brain/awr148

Nicot, A. S., & Laporte, J. (2008). Endosomal phosphoinositides and human diseases. *Traffic*, *9*(8), 1240–1249. https://doi.org/10.1111/j.1600-0854.2008.00754.x

Odorizzi, G., Babst, M., & Emr, S. D. (2000). Phosphoinositide signaling and the regulation of membrane trafficking in yeast. *Trends in Biochemical Sciences*, *25*(5), 229–235. https://doi.org/10.1016/S0968-0004(00)01543-7

Piao, X., Hill, R. S., Bodell, A., Chang, B. S., Basel-vanagaite, L., Straussberg, R., Dobyns, W. B., Qasrawi, B., Winter, R. M., Innes, A. M., Voit, T., Ross, M. E., Michaud, J. L., & Walsh, C. A. (2004). *G Protein–Coupled Another approach to studying the mecha- nisms of cortical specification can come from the genetic analysis of inherited conditions in Receptor–Dependent Development which specific regions of the cortex are prefer- entially disrupted. Bil*.

Pryor, P. R., & Luzio, J. P. (2009). Delivery of endocytosed membrane proteins to the lysosome. *Biochimica et Biophysica Acta - Molecular Cell Research*, *1793*(4), 615–624. https://doi.org/10.1016/j.bbamcr.2008.12.022

Pulvirenti, T., Giannotta, M., Capestrano, M., Capitani, M., Pisanu, A., Polishchuk, R. S., Pietro, E. S., Beznoussenko, G. V., Mironov, A. A., Turacchio, G., Hsu, V. W., Sallese, M., & Luini, A. (2008). A traffic-activated Golgi-based signalling circuit coordinates the secretory pathway. *Nature Cell Biology*, *10*(8), 912–922. https://doi.org/10.1038/ncb1751

Rink, J., Ghigo, E., Kalaidzidis, Y., & Zerial, M. (2005). Rab conversion as a mechanism of progression from early to late endosomes. *Cell*, *122*(5), 735–749. https://doi.org/10.1016/j.cell.2005.06.043

Ron, D., & Walter, P. (2007). Signal integration in the endoplasmic reticulum unfolded protein response. *Nature Reviews Molecular Cell Biology*, *8*(7), 519–529. https://doi.org/10.1038/nrm2199

Rothman, J. E. (2002). The machinery and principles of vesicle transport in the cell. *Nature Medicine*, *8*(10), 1059–1062. https://doi.org/10.1038/nm770

Saporta, A. S. D., Sottile, S. L., Miller, L. J., Feely, S. M. E., Siskind, C. E., & Shy, M. E.

(2011). Charcot-marie-tooth disease subtypes and genetic testing strategies. *Annals of Neurology*, *69*(1), 22–33. https://doi.org/10.1002/ana.22166

Sbrissa, D., Ikonomov, O. C., Fenner, H., & Shisheva, A. (2008). ArPIKfyve Homomeric and Heteromeric Interactions Scaffold PIKfyve and Sac3 in a Complex to Promote PIKfyve Activity and Functionality. *Journal of Molecular Biology*, *384*(4), 766–779. https://doi.org/10.1016/j.jmb.2008.10.009

Sbrissa, D., Ikonomov, O. C., Fu, Z., Ijuin, T., Gruenberg, J., Takenawa, T., & Shisheva, A. (2007). Core protein machinery for mammalian phosphatidylinositol 3,5-bisphosphate synthesis and turnover that regulates the progression of endosomal transport: Novel Sac phosphatase joins the ArPIKfyve-PIKfyve complex. *Journal of Biological Chemistry*, *282*(33), 23878–23891. https://doi.org/10.1074/jbc.M611678200

Schekman, R., & Rothman, J. E. (2002). Dissecting the membrane trafficking system. *Nature Medicine*, *8*(10), 1055–1058. https://doi.org/10.1038/nm769

Schreij, A. M. A., Fon, E. A., & McPherson, P. S. (2016). Endocytic membrane trafficking and neurodegenerative disease. *Cellular and Molecular Life Sciences*, *73*(8), 1529–1545. https://doi.org/10.1007/s00018-015-2105-x

Shewan, A., Eastburn, D. J., & Mostov, K. (2011). Phosphoinositides in cell architecture. *Cold Spring Harbor Perspectives in Biology*, *3*(8), 1–17. https://doi.org/10.1101/cshperspect.a004796

Simon A. Rudge, Deborah M. Anderson, and S. D. E. (2004). Vacuole Size Control: Regulation of PtdIns(3,5)P2 Levels by the Vacuole-associated Vac14-Fig4 Complex, a PtdIns(3,5)P2-specific Phosphatase. *Molecular Biology of the Cell*, *15*(January), 5069–5081. https://doi.org/10.1091/mbc.E03

Stenmark, H. (2003). Phosphoinositides in subcellular targeting and enzyme activation: Preface. In *Current Topics in Microbiology and Immunology* (Vol. 282).

Tazir, M., Bellatache, M., Nouioua, S., & Vallat, J. M. (2013). Autosomal recessive Charcot-Marie-Tooth disease: From genes to phenotypes. *Journal of the Peripheral Nervous System*, *18*(2), 113–129. https://doi.org/10.1111/jns5.12026

Vaccari, I., Carbone, A., Previtali, S. C., Mironova, Y. A., Alberizzi, V., Noseda, R., Rivellini, C., Bianchi, F., Del Carro, U., D'Antonio, M., Lenk, G. M., Wrabetz, L., Giger, R. J., Meisler, M. H., & Bolino, A. (2014). Loss of Fig4 in both Schwann cells

and motor neurons contributes to CMT4J neuropathy. *Human Molecular Genetics*, *24*(2), 383–396. https://doi.org/10.1093/hmg/ddu451

Valence, S., Poirier, K., Lebrun, N., Saillour, Y., Sonigo, P., Bessières, B., Attié-Bitach, T., Benachi, A., Masson, C., Encha-Razavi, F., Chelly, J., & Bahi-Buisson, N. (2013). Homozygous truncating mutation of the KBP gene, encoding a KIF1B-binding protein, in a familial case of fetal polymicrogyria. *Neurogenetics*, *14*(3–4), 215–224. https://doi.org/10.1007/s10048-013-0373-x

Varghese, P., Collins, N., Warner, G., Leitch, J., Ho, E., & Crock, P. (2014). Yunis-Varon syndrome: Further delineation of cardiovascular and endocrine outcome. *American Journal of Medical Genetics, Part A*, *164*(5), 1213–1217. https://doi.org/10.1002/ajmg.a.35741

Vembar, S. S., & Brodsky, J. L. (2008). One step at a time: Endoplasmic reticulum-associated degradation. *Nature Reviews Molecular Cell Biology*, *9*(12), 944–957. https://doi.org/10.1038/nrm2546

Vicinanza, M., D'Angelo, G., Di Campli, A., & De Matteis, M. A. (2008). Function and dysfunction of the PI system in membrane trafficking. *EMBO Journal*, *27*(19), 2457–2470. https://doi.org/10.1038/emboj.2008.169

Vonderheit, A., & Helenius, A. (2005). Rab7 associates with early endosomes to mediate sorting and transport of Semliki forest virus to late endosomes. *PLoS Biology*, *3*(7), 1225–1238. https://doi.org/10.1371/journal.pbio.0030233

Walch, E., Schmidt, M., Brenner, R. E., Emons, D., Dame, C., Pontz, B., Wiestler, O. D., & Bartmann, P. (2000). Yunis-Varon syndrome: Evidence for a lysosomal storage disease. *American Journal of Medical Genetics*, *95*(2), 157–160. https://doi.org/10.1002/1096-8628(20001113)95:2<157::AID-AJMG12>3.0.CO;2-E

Watson, P., & Stephens, D. J. (2005). ER-to-Golgi transport: Form and formation of vesicular and tubular carriers. *Biochimica et Biophysica Acta - Molecular Cell Research*, *1744*(3 SPEC. ISS.), 304–315. https://doi.org/10.1016/j.bbamcr.2005.03.003

Waugh, M. G. (2015). PIPs in neurological diseases. *Biochimica et Biophysica Acta - Molecular and Cell Biology of Lipids*, *1851*(8), 1066–1082. https://doi.org/10.1016/j.bbalip.2015.02.002

Whiteford;, C. C., Brearley;, C. A., & Ulug, E. T. (1997). *in Resting Mouse Fibroblasts*.

601, 597–601.

Winter, E. E., Goodstadt, L., & Ponting, C. P. (2004). Elevated rates of protein secretion, evolution, and disease among tissue-specific genes. *Genome Research*, *14*(1), 54–61. https://doi.org/10.1101/gr.1924004

Yamamoto, A., DeWald, D. B., Boronenkov, I. V., Anderson, R. A., Emr, S. D., & Koshland, D. (1995). Novel PI(4)P 5-kinase homologue, Fab1p, essential for normal vacuole function and morphology in yeast. *Molecular Biology of the Cell*, *6*(5), 525–539. https://doi.org/10.1091/mbc.6.5.525

Yin, H. L., & Janmey, P. A. (2003). Phosphoinositide Regulation of the Actin Cytoskeleton. *Annual Review of Physiology*, *65*(1), 761–789. https://doi.org/10.1146/annurev.physiol.65.092101.142517

Zhang, Xiaoli, Li, X., & Xu, H. (2012). Phosphoinositide isoforms determine compartment-specific ion channel activity. *Proceedings of the National Academy of Sciences of the United States of America*, *109*(28), 11384–11389. https://doi.org/10.1073/pnas.1202194109

Zhang, Xuebao, Chow, C. Y., Sahenk, Z., Shy, M. E., Meisler, M. H., & Li, J. (2008). Mutation of FIG4 causes a rapidly progressive, asymmetric neuronal degeneration. *Brain*, *131*(8), 1990–2001. https://doi.org/10.1093/brain/awn114

Zhang, Y., Zolov, S. N., Chow, C. Y., Slutsky, S. G., Richardson, S. C., Piper, R. C., Yang, B., Nau, J. J., Westrick, R. J., Morrison, S. J., Meisler, M. H., & Weisman, L. S. (2007). Loss of Vac14, a regulator of the signaling lipid phosphatidylinositol 3,5-bisphosphate, results in neurodegeneration in mice. *Proceedings of the National Academy of Sciences of the United States of America*, *104*(44), 17518–17523. https://doi.org/10.1073/pnas.0702275104

Annex 1 – Calibration curve for Bradford assay

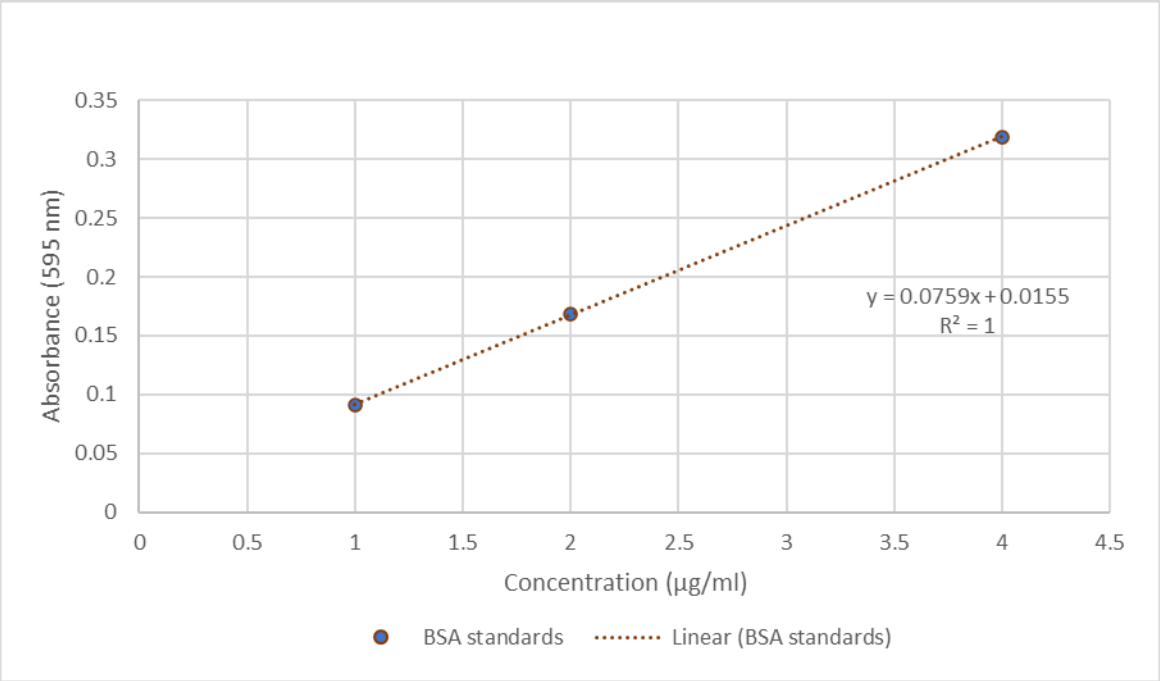

Figure 12 - Calibration curve with BSA standards (1, 2 and 4 µg/ml), to determine protein concentration in cells lysate in Bradford assay at 595 nm

Annex 2 – Western blot analysis on LAMP-1 and EEA1 of cells lysates

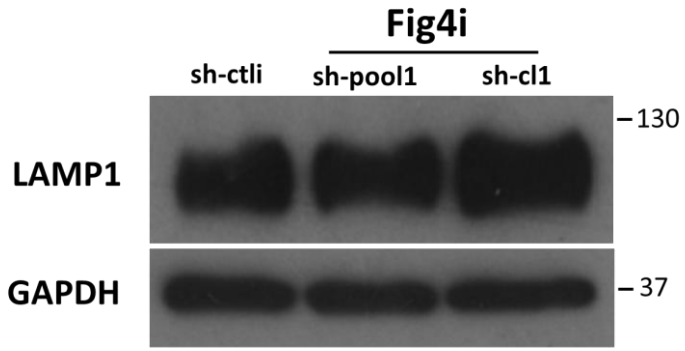

Figure 13 - Ctli and Fig4i cells were immunoblotted with an anti-Lamp1 antibody; GAPDH was used as loading control. Molecular weights of proteins are indicated (lysates obtained from different cultures)

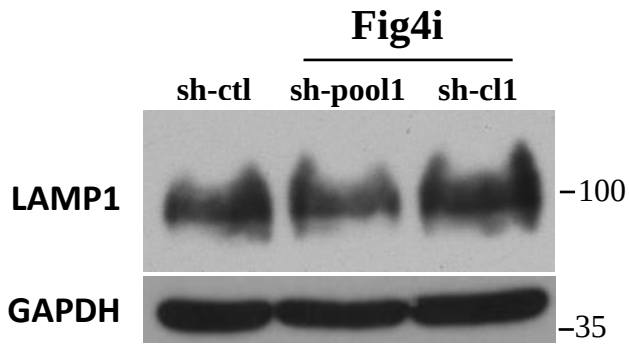

Figure 14 - Ctli and Fig4i cells were immunoblotted with an anti-Lamp1 antibody; GAPDH was used as loading control. Molecular weights of proteins are indicated (lysates obtained from different cultures)

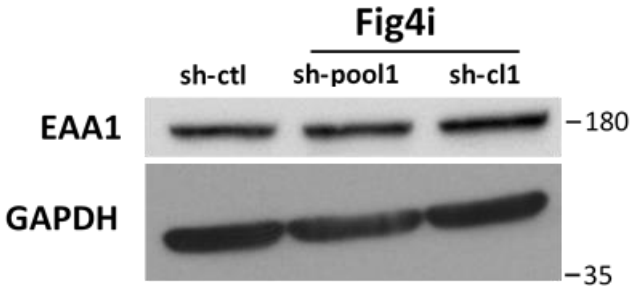

Figure 15 - Ctli and Fig4i cells were immunoblotted with an anti-EEA1 antibody; GAPDH was used as loading control. Molecular weights of proteins are indicated (lysates obtained from different cultures)

Annex 3 – Growth curve of Fig4i cells

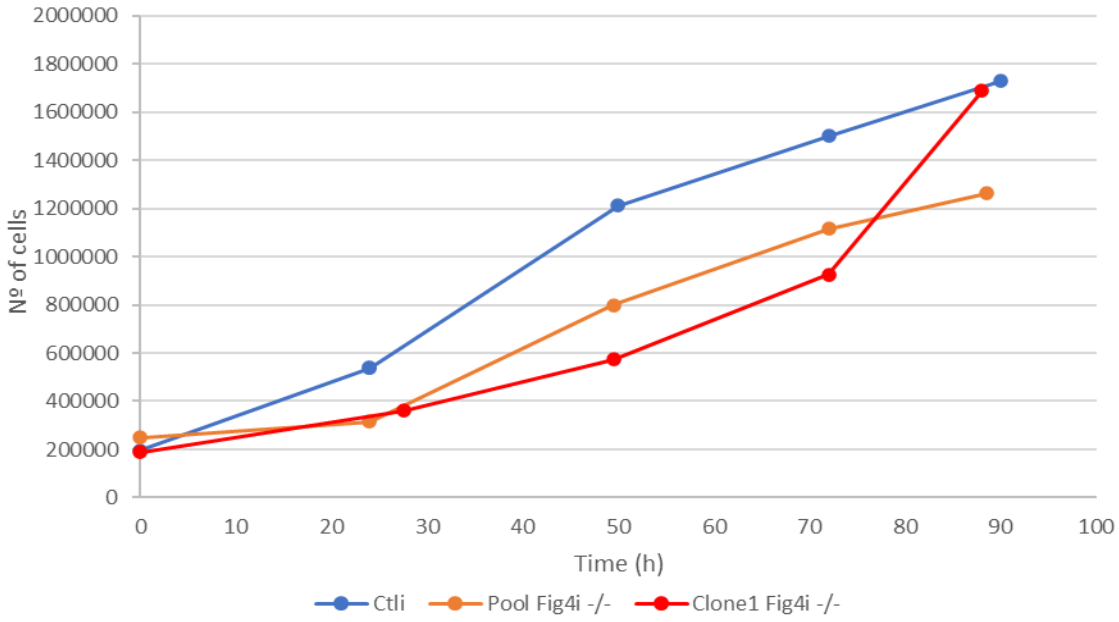

Figure 16 - Ctli and Fig4i were seeded on 60mm diameter dishes the cell growth was monitored counting every 24 hours. Representative growth curves are shown in the graphic